Hydrophobins from *Aspergillus* mediate fungal interactions with microplastics

Ross R. Klauer[1], Rachel Silvestri[1], Hanna White[1], Milton Das[2], Richard D. Hayes[3], Robert Riley[3], Anna Lipzen[3], Kerrie Barry[3], Igor V. Grigoriev[3,4], Jayson Talag[5], Victoria Mae Bunting[5], Zachary Stevenson[1], Philip Demokritou[2], Kevin V. Solomon[1]*, Mark Blenner[1]*

1 Chemical and Biomolecular Engineering, University of Delaware, 150 Academy St., Newark, DE 19716.
2 Nanoscience and Advanced Materials Center, Environmental and Occupational Health Sciences Institute, Rutgers University, 170 Frelinghuysen Road, Piscataway, New Jersey 08854
3U.S. Department of Energy Joint Genome Institute, Lawrence Berkeley National Laboratory, Berkeley, CA 94720
4 Department of Plant and Microbial Biology, University of California Berkeley, Berkeley, CA 94720
5 Arizona Genomics Institute, 1657 E Helen St, Tucson, AZ 85721

**Equal contribution, corresponding authors.*
Correspondence: blenner@udel.edu; kvs@udel.edu

Abstract:

Microplastics cause negative environmental consequences such as the release of toxic additive leachates, increased greenhouse gas emissions during degradation, and threaten food chains . Microplastic particles are known to serve as a vector for transport of microbes (fungi and bacteria) to new environments, threatening biodiversity. Robust biofilm formation makes fungi a candidate to collect and remediate environmental microplastics. However, fungal-microplastic colonization mechanisms have yet to be explored. In this work, we aim to understand which fungal molecules mediate microplastics binding. We examine common fungal genus *Aspergillus* , which we found binds microplastics tightly, removing particles from suspension. Upon inoculation of *Aspergilli* with microplastics particles, up to 3.85 +/- 1.48 g of microplastics were flocculated per gram of dry fungal biomass; this phenomenon was observed across various plastics ranging in size from 0.05 – 5 mm. Gene knockouts revealed that hydrophobins drive microplastic-fungi binding, evidenced by a decrease in flocculation relative to wild-type *Aspergillus fumigatus*. Moreover, purified hydrophobins flocculated microplastics independently of the fungus, validating their ability to bind to microplastics. Our work elucidates a role for hydrophobins in fungal colonization of microplastics and highlights a target for mitigating the harm of microplastics through engineered fungal-microplastic interactions.

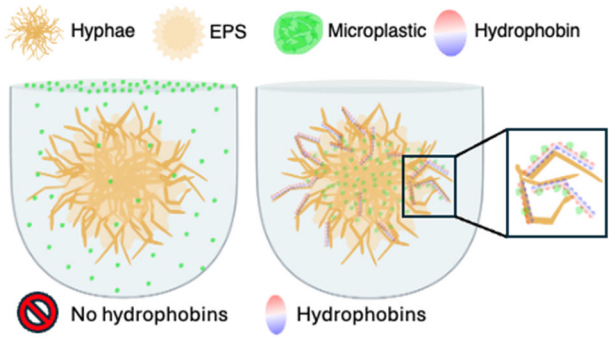

Keywords: hydrophobin, microplastic, fungi, flocculation

Synopsis: Aspergillus bind microplastics via hydrophobin proteins that may be used as a capture agent to mitigate microplastics pollution in oceans and waterways.

Introduction:

Microplastics accumulation in the environment has led to myriad environmental, biodiversity, and human health issues[1–7] . An estimated 275 million tons of plastic are disposed at end of life each year[8],with the majority of these plastics degraded into microplastic particles dispersed in our air, water, and soils[9]. Their presence in the environment leads to the release of toxic xenobiotics through additive leaching[10], and increases in greenhouse gas levels from environmental microplastics degradation and toxicity to phytoplankton that fix atmospheric CO_2[11]. Microplastic particles present negative environmental consequences worldwide, as they are found ubiquitously in soil, groundwater, marine environments, estuaries, and landfills due to their low density and small size that allows them to easily be carried to new locations[12]. As a result of this rapid transport, microplastics with biofilm-bound microbes are often transported to new environments, leading to disruption of the local microenvironment through the introduction of new, possibly invasive or pathogenic, species[13]. Moreover, microplastic particles have been observed in the intestinal tracts, tissues, and organs of marine organisms throughout the ecosystem[14] and have been shown to lead to negative health consequence in mice, zebrafish, and other animals such as inflammation, metabolic disorders, and decreases in reproduction[13]. Microplastic particles subsequently work their way through animal and human food chains, potentially exacerbating these negative health effects through the entire food web, threatening biodiversity[15]. Consequently, microplastics have been found in human placentas[16], testes[17], and blood[18] leading to negative health effects from leaching of toxic monomers, additives, and adsorbed environmental pollutants[19–23]. More importantly, polyethylene microplastics in human arteries increase the likelihood of cardiovascular events, stroke, or death[24]. These environmental and human health issues continue to worsen with exponential increases in plastic production and subsequent increases in environmental contamination[25].

Microorganisms frequently interact with microplastics, forming robust biofilms on their surface. These biofilms lead to the transport of new microbes to foreign environments, disrupting the local ecosystem and food chains[12,26]. Moreover, microplastic biofilms are often enriched in pathogens such as those from the genera *Pseudomonas*[27,28] and *Vibrio*[28]. Pathogens tend to be enriched in biofilms due to their ability to promote cell fitness via horizontal gene transfer of antibiotic resistance genes that improve microbial viability of other members of the microbial community[29]. Additionally, pathogens such as *Vibrios* have been noted to evolve into hyperbiofilm-formers in stressed microenvironments[29]. The presence and enrichment of pathogenic microbes in these biofilms can exacerbate animal health, biodiversity, and human health impacts by introducing new pathogens into microbial communities and food chains and by harboring increased horizontal transfer of antibiotic resistance genes between pathogens[27,28,30]. Such pathogenic consequences are evidenced by disease outbreaks in marine environments tied to the migration of pathogens on plastics waste[31,32]. The taxonomic profiles of microplastic-associated biofilms are well documented[33–35], as taxonomic changes to biofilm members vary dependent on sampling location, plastic type, and particle size[33,36,37]. While there is a strong understanding of the types of microorganisms that bind to microplastic particles under various conditions, the specific biomolecules responsible for microbial binding to microplastics are poorly understood.

Microbes often form biofilms on solid surfaces through secretion of biosurfactants and/or surface proteins. For example, bacteria often rely on flagella or pili to attach to surfaces and form biofilms[38,39]. Additionally, many bacteria secrete extracellular polymeric substances (EPS) containing proteins and lipopolysaccharides (LPS) that promote biofilm hydrophobicity and allow for surface binding[40]. Similarly, fungal adhesion to extracellular surfaces is canonically driven by surface proteins called adhesins[41]. Adhesins are responsible for cell-cell adhesion, biofilm formation, and adhesion to hydrophobic surfaces in model yeasts like *S. cerevisiae*[42]. Common

fungi such as *Aspergilli* secrete adhesins belonging to the class hydrophobins that allow them to form strong hyphal networks and adhere to extracellular surfaces[43]. Hydrophobins are a class of small, secreted fungal proteins (~10-15kDa) that form amphipathic layers at hydrophobic/hydrophilic interfaces[43], allowing them to bridge fungi to extremely hydrophobic substrates. Though they are known to form strong biofilms on solid surfaces, the interactions of fungi with (micro)plastics are understudied. However, there is growing interest in the fungal members of microplastic-associated biofilms and their interactions due to the inherent pathogenicity of many fungi and their propensity for horizontal gene transfer[36,44]. *Aspergillus niger* has been documented to interact with and bind to polystyrene (PS) and Poly(methyl methacrylate) (PMMA), removing PS and PPMA from solution[45], but binding mechanisms were not studied. These fungi-microplastics relationships are essential to understand how microplastics are colonized, mitigation of health risks from microplastic-bound pathogenic fungi, potential toxicity effects, and how to better remove microbes from microplastics for recovery.

In this study, we leverage *Aspergillus fumigatus* to better understand the manner in which fungi bind to microplastics because it is a reported opportunistic pathogen and is found ubiquitously across soil and marine environments[46,47]. We isolated a novel strain of *Aspergillus fumigatus* that forms extremely hydrophobic biofilms, recovering nearly 100% of microplastics from suspensions. These observations, concurrent with those found in *A. niger,* imply that there is a conserved mechanism across all *Aspergilli* for microplastics binding. Our observations of microplastics flocculation across several strains covering the genus phylogeny validate this hypothesis. Moreover, we confirmed that microplastics recovery occurs ubiquitously across various single and mixed plastic types, demonstrating that fungal-microplastics interactions are conserved on model post-consumer plastic waste streams. We hypothesized that microplastics bind to hydrophobins on *Aspergilli* hyphae due to their abundance and ubiquity across the genus and due to their inherent hydrophobicity[43,48,49]. Additionally, hydrophobins have been reported to bind to and enhance enzymatic plastics deconstruction [50]. For example, RolA from *A. oryzae* has been reported to bind to polybutylene succinate-coadipate and recruit esterases for its deconstruction[51,52] and hydrophobins have been used to enhance enzymatic PET hydrolysis[50]. Here, we show that hydrophobin proteins from *A. fumigatus* are the primary driver for microplastic binding by *Aspergillus* through gene knockouts and confirming pure hydrophobin binding to microplastic particles. The understanding that hydrophobins are responsible for microplastic binding can be used to reverse biofilm formation by pathogenic strains such as *Aspergillus fumigatus*, subsequently mitigating potential pathogenicity of microplastics, reducing negative health effects on animals. Additionally, hydrophobins can be used in the absence of (pathogenic) hosts to provide sustainable microplastics recovery from aqueous environments, alleviating negative consequences to biodiversity.

Materials and methods:

Organism Isolation: *Aspergillus fumigatus* AF-UD1 was isolated from the gut of a yellow mealworm (*Tenebrio* molitor larvae) fed HDPE for 20 days. 10 mealworm guts were extracted, suspended in 1 mL of PBS, and vortexed to homogenize. 50 µL of gut contents were plated on fungal Medium B (defined previously[53]). Individual colonies were re-plated on Medium B to isolate the organism. The organism was originally isolated in a co-culture with an un-identified bacterial strain. AF-UD1 was isolated from the co-culture by plating on potato dextrose agar with 50 µg/mL penicillin and 50 µg/mL streptomycin.

Organism Identification: Whole genome sequencing was carried out on genomic DNA from AF-UD1, with details of each method outlined below.

DNA Extraction: High molecular weight DNA was extracted from mycelium using the protocol of Puppo et al (2017)[54] with minor modifications. Flash-frozen biomass was ground to a fine powder in a frozen mortar with liquid nitrogen followed by very gentle extraction in 3X CTAB extraction buffer (3% CTAB (hexadecyltrimethylamonium bromide), 1.4 M NaCl, 100 mM Tris pH 8.0, 20 mM EDTA, 1% 2-mercaptoethanol) for 1h at 65 °C. The mixture was cooled down and gently extracted with 24:1 Chloroform:Isoamyl alcohol. The upper phase was collected and gently extracted again with 24:1 Chloroform:Isoamyl alcohol. The aqueous phase was transferred to a new tube and 1/10th volume 3 M Sodium acetate was added, gently mixed, before precipitating the DNA with iso-propanol. The sample was kept in -20 °C overnight to facilitate precipitation. DNA precipitate was collected by centrifugation, washed with 70% ethanol, air dried for 5 minutes and dissolved thoroughly in elution buffer at room temperature followed by RNAse treatment. DNA purity was measured with Nanodrop, DNA concentration measured with Qubit HS kit (Invitrogen) and DNA size was validated by Femto Pulse System (Agilent).

Genome Sequencing: The draft genome of AF-UD1 was sequenced using PacBio Multiplexed 6-10kb Ultra-Low Input library sequenced using the REVIO. An input of 50 ng of genomic DNA was sheared to 6 kb - 10 kb using the Megaruptor® 3 (Diagenode) or g-TUBE (Covaris). The sheared DNA was treated with DNA damage repair enzyme mix, end-repair/A-tailing mix and ligated with amplification adapters using SMRTbell Express Template Prep Kit 3.0 (PacBio) and purified with SMRTbell cleanup beads. The purified ligation product was split into two reactions and enriched using 10-18 cycles of PCR using barcoded amplification oligos (IDT) and SMRTbell® gDNA Sample Amplification Kit (PacBio). Up to sixteen libraries were pooled in equimolar concentrations and the pooled libraries were size-selected using the 0.75% agarose gel cassettes with Marker S1 and High Pass protocol on the BluePippin (Sage Science). The size-selected pools were treated with DNA damage repair enzyme mix, end-repair/A-tailing mix and ligated with SMRTbell sequencing adapters, a nuclease enzyme mix and purified with SMRTbell cleanup beads. CCS data was filtered with the JGI QC pipeline to remove artifacts. CCS reads were assembled with Flye version 2.9-b1768 (https://github.com/fenderglass/Flye) and subsequently polished with two rounds of RACON version 1.4.13 [55]. The mitochondrial sequence was identified based on coverage, GC content, and BLAST hits to the NCBI nt database, used to filter the CCS reads to produce non-organelle CCS, and polished with two rounds of RACON version 1.4.13[55].

Gene calling was facilitated through transcriptome acquisition and a single RNA-seq library was produced as input for the Joint Genome institute (JGI) annotation pipeline. The JGI gene finding methods include the use of filtered reads, or trinity-assembled contigs as transcriptional evidence that the gene is translated. mRNA was isolated from an input of 200 ng of total RNA with oligo dT magnetic beads and fragmented to 300 bp - 400 bp with divalent cations at a high temperature. Using the TruSeq stranded mRNA kit (Illumina), the fragmented mRNA was reverse transcribed to create the first strand of cDNA with random hexamers and SuperScript™ II Reverse Transcriptase (Thermo Fisher Scientific) followed by second strand synthesis. The double stranded cDNA fragments were treated with A-tailing, ligation with NEXTFLEX UDI Barcodes (PerkinElmer) and enriched using 10 cycles of PCR. The prepared libraries were quantified using KAPA Biosystems' next-generation sequencing library qPCR kit and run on a Roche LightCycler 480 real-time PCR instrument. Sequencing of the flowcell was performed on the Illumina NovaSeq sequencer using NovaSeq XP V1.5 reagent kits, S4 flowcell, following a 2x151 indexed run recipe. RNA-Seq reads were trimmed for artifact sequence by kmer matching (kmer=25), allowing 1 mismatch, from the 3' end of the reads, and filtered for spike-in reads, PhiX reads and reads containing any Ns.

Quality trimming of the genome was performed using the phred trimming method set at Q6. Finally, following trimming, reads under the length threshold were removed (minimum length 25 bases or 1/3 of the original read length - whichever is longer). Filtered reads were assembled into consensus sequences using Trinity v2.12.0[56]. The genome was annotated using the JGI Annotation pipeline and made publicly available via JGI fungal genome portal MycoCosm[57]. The genome is available on JGI MycoCosm at https://mycocosm.jgi.doe.gov/AspfumUD1_1/AspfumUD1_1.info.html

Protein Clustering and Phylogenetic Analysis: *Aspergillus* species below were downloaded from MycoCosm and included in orthofinder v2.55 clustering with *A. fumigatus* UD1[58]. Briefly, all GeneCatalog proteins were clustered into orthologous groups (orthogroups) by sequence similarity. A total of 5345 orthogroups contained every species, and were aligned to produce a species tree using default methods[59,60]. The tree file was plotted along with MycoCosm assembly and gene count metrics by phytools[61]. Genome references are original publications unless sourced from AspGD[62]: *A. flavus* NRRL 3357[63]; *A. fischeri* NRRL 181[62]; *A. fumigatus* Af293[64]; *A. fumigatus* A1123[65]; *A. nidulans* FGSC A4[62]; *A. niger* NRRL3[66]; *A. novofumigatus* IBT 16806[67]; *A. terreus* NIH 2624[62]; *A. udagawae* IFM 46973[68]

Microplastics recovery assays: *Aspergillus* pre-cultures were grown in YPD at 37 °C, 220 rpm in 5 mL cultures for 2 days directly from a freezer stock. The pre-culture was then inoculated into 100 mL YPD to and grown at 37 °C, 100 rpm in a 500 mL flask to grow *Aspergillus* 'flocs' of LDPE (Goodfellow Cambridge Limited, Huntingdon, England; catalog number LS563303), PP **(**post-consumer yogurt Chobani yogurt cups; PP disks/beads cut out using a 2 mm diameter hole punch), PET (post-consumer Dasani water bottles; PET disks/beads cut out using a 5 mm diameter hole punch), or UHMWPE (Sigma-Aldrich Chemical Company; catalog number 43272 – 100g). Or, cellulose acetate (0.45 µm, Sterlitech corporation, Auburn, WA, USA; catalog number CA0459025) used in place of microplastic particles. In addition, environmentally relevant cryomilled and UV weathered PVCmicronanoplastics with an average size of 5 um, were provided by the Rutgers Nanoscience and Advanced Materials Center and used [69]. Details on their synthesis and physicochemical properties are summarized in the Suppl. information section and detailed by the authors in the Das et al publication[61]). Approximately 25 mg microplastics (or cellulose acetate) particles were suspended in 5 mL of sterile mineral media (1g NaH_2PO_4, 0.5 g $MgSO_4*7H_2O$, 0.2 g KH_2PO_4, and 1 g yeast extract per 1 liter). 2-3 flocs from the large *Aspergillus* culture were dropped into the 5 mL culture containing plastic powder or disks. The cultures were allowed to shake at 30 °C, 220 rpm to allow the *Aspergillus* strains to slowly grow in a nutrient deprived environment. Every 2 hours, the culture was shaken to allow fungi to come into direct contact with the plastic. Once plastic was flocculated at one of these 2 hour intervals, the culture was removed for analysis. If no plastic was grabbed by the fungi (in the case of *Aspergillus* knockout experiments) after 36 hours, the culture was removed and discarded.

For mass-normalized microplastics recovery assays, flocs of *A. fumigatus* UD01, *A. fumigatus* (ATCC 1022), *A. niger* (ATCC 16888), *A. nidulans* (ATCC10074), *A. flavus* (ATCC 16833), or *A. terreus* (ATCC 1012) containing microplastics were removed from the culture tubes using sterile weighing spatulas onto pre-weighed dishes and allowed to dry. Remaining plastic was subsequently removed from the tube by flushing the tube with water and ensuring all remaining contents of the tube were deposited onto a pre-weighed dish. Both pre-weighed dishes were then weighed after drying. Mass of flocculated plastic was calculated by subtracting the mass of remaining plastic from the initial plastic mass. Additionally, the microplastic-flocculated cultures were weighed. Calculated flocculated plastic mass was subtracted from the mass of the dried flocculated plastic fungal culture to obtain dry biomass weight.

For microplastics recovery assays that included beta-mercaptoethanol (βME), the βME was added into the culture tube with plastic and prior to adding the fungal flocs. Flocs were added and the protocol outlined above was followed.

For recovery assay with pure RodA, 10 mg of green fluorescent LDPE particles (Cospheric LLC, Somis, CA; catalog number UVPMS-BG-1.00 35-45 um) were placed into 1 mL of solution containing purified RodA. The solution was lightly shaken to mix and then left stationary at room temperature overnight to allow separation.**Preparation of weathered PVC (w-PVC) particles:** Methods for weathering and materials testing of w-PVC particles can be found in Supplementary information file 2. Particles were prepared via methods in ref. [69]

Confocal microscopy: Microplastics recovery assays were carried out as above, but with red fluorescent LDPE beads (Cospheric LLC, Somis, CA; catalog number UVPMS-BR-0.995 45-53 um). After flocculation, floc culture was washed with PBS three times. The culture was placed into a microscopy sample dish (ibidi ibiTreat: #1.5 polymer coverslip, tissue culture treated, sterilized) in 2 mL PBS. One microliter of calcofluor white was added to the culture and it was stored in darkness for 15 minutes to stain the fungi. Microscopy images were taken using a Stellaris 8 tauSTED/FLIM Confocal Microscope at the University of Delaware Bioimaging Center.

Scanning electron microscopy: Microplastics recovery assays were carried out as above. After flocculation, floc culture was washed with PBS three times. Culture flocs were coated in platinum and imaged on the Apreo VolumeScope™ Scanning Electron Microscope at the University of Delaware Bioimaging Center.

Hydrophobin knockout strains: Mutant hydrophobin knockout strains were generously donated by Jean-Paul Latgé and Isabelle Mouyna from Aspergillus Unit, Institut Pasteur, 75015 Paris, France. The hydrophobin knockouts were generated from methods listed in the original publication[43].

RodA cloning in *Yarrowia lipolytica*: RodA sequence was codon optimized for *Yarrowia lipolytica* and the resulting gene fragment was ordered from Twist Biosciences with an AscI restriction site on the N terminus and an NheI restriction site on the C terminus. The gene fragment was digested with AscI and NheI enzymes at 37 °C for 1 hour and then therestriction enzymes were heat inactivated at 80 °C for 20min. The vector for cloning was a homology donor for integration into the AXP site in Yarrowia lipolytica[70]. The vector was also digested with AscI and NheI at 37 °C for 1 hour. The vector and insert were ligated using NEB DNA ligase. 5uL of ligation mix was added to 50 µL of NEB 10β competent cells which were heat shocked at 42 °C for 30 seconds and then recovered in 1mL of LB media for 1 hour at 37ºC with shaking. 100 µL of transformed cells were plated onto an ampicillin containing LB plate and grown overnight at 37 °C. The sequence of the resulting plasmid was confirmed by Sanger sequencing. The RodA gene was integrated into the AXP site using the homology donor and a CRISPR containing plasmid. Integration was confirmed via colony PCR and then the strain was cured of all plasmids.

RodA expression and purification: *Yarrowia lipolytica* RodA was grown for 4 days at 28ºC with agitation at 220 rpm in 50 mL YPD. Culture was transferred to 50 mL falcon tube and centrifuged at 4000 rpm to separate pellet and supernatant. Supernatant was ultra-centrifuged for 1hr at 100,000g in SW32Ti rotor using OptiSeal 32mL tubes and adapters from Beckman Coulter. Supernatant was removed and pellet was resuspended in 1 mL of 2% SDS. The sample was transferred to microcentrifuge tube and boiled for 10 min at 98 °C. In 5mL thinwall open top tubes (Bechman Coulter), sample was ultra-centrifuged at 100,000 g in 5 mL of SDS for 1 hr at 20 °C. This process was repeated 2 times. All SDS was removed and the pellet was resuspended in

5mL DI water. The sample was then ultra-centrifuged at 100,000 g for 1 hr at 20 °C. This process was repeated 2 times. Resulting hydrophobin pellet was transferred to a 1.5 mL microcentrifuge tube with 1mL DI water. RodA expression and purification protocol was adapted from[71]. Purified RodA was then ran on a tris-trycine SDS-PAGE gel stained with silver stain using concentrations found in Supplementary Table 1 calculated via BCA assay. Purity was confirmed via SDS-PAGE gel (Supplementary Figure 3) that shows a dominant band in RodA culture supernatant after going through the purification process. This band is not present in the wild type strain (Supplementary Figure 3).**Results:**

A novel microbial isolate from the yellow mealworm gut microbiome flocculates microplastics from suspension

We discovered a microbial isolate from the gut of *Tenebrio molitor* that flocculates microplastics, pulling them out of suspension. The isolate rapidly flocculated suspended ultra-high molecular weight polyethylene (UHMWPE) particles and floating red fluorescent LDPE particles within seconds (Fig. 1A). Moreover, fungal-microplastics flocs are highly stable in solution; we observed that microplastics remain bound to fungi at 4°C and at room temperature for up to 6 months after conclusion of flocculation experimentation (data not shown). We evaluated the extent of microplastics flocculation capabilities of this isolate by using 25 mg (0.4% wt./vol) polypropylene (PP), poly(ethylene terephthalate) (PET), surface oxidized UHMWPE, and low-density polyethylene (LDPE) plastics to ensure that the strain can bind to microplastics independent of polymer chemistry and hydrophobicity. 25 mg/mL was selected as it is well above the range of reported microplastics concentrations of 1 – 2000 mg/L reported from marine and wastewater environments[72,73] and can be reliably measured in the laboratory. The isolate captured 96.0 +/- 4.0% of 200 µm LDPE particles, 97.1 +/- 0.6% of 50 µm UHMWPE particles, 100 +/- 0% of 5 mm PET beads, and 90.9 +/- 8.1% of 2 mm PP beads meaning flocculation is independent of both polymer chemistry and particle size (Fig. 1B). Mixed plastic types did not interfere with flocculation. Pairwise combinations of plastics were still recovered with 85-100% efficiency and 92% recovery when a 40 mg (0.8% wt. vol) mixture of all 4 microplastic types and sizes was tested (Fig. 1B). These combinatorial samples were performed as they more closely emulate the mixed microplastics streams that occur in marine environments. Samples containing PP and PET beads have higher variance due to their larger particle size. If one PP or PET bead was not recovered, it significantly decreases the plastic recovery on the per mass basis. It is likely that the increased surface area of the larger particles requires more binding interactions to retain the plastic within the biofilm, leading to some particles not being captured due to lack of available fungal surface area. Nonetheless, microplastics flocculation is nearly 100% in both ‘pure’ and mixed plastic cases, with pristine and post-consumer plastics of varying chemistries and sizes. Additionally, the flocculation phenotype is maintained upon plastics UV photooxidation and weathering, as ~5 µm weathered PVC particles[69] were recovered with a mass yield similar to PP beads (Supplementary Fig. 1). Lastly, the flocculation phenotype was also conserved when repeating assays using cellulose acetate, suggesting that the binding phenotype is not plastic-specific (Supplementary Fig. 2).

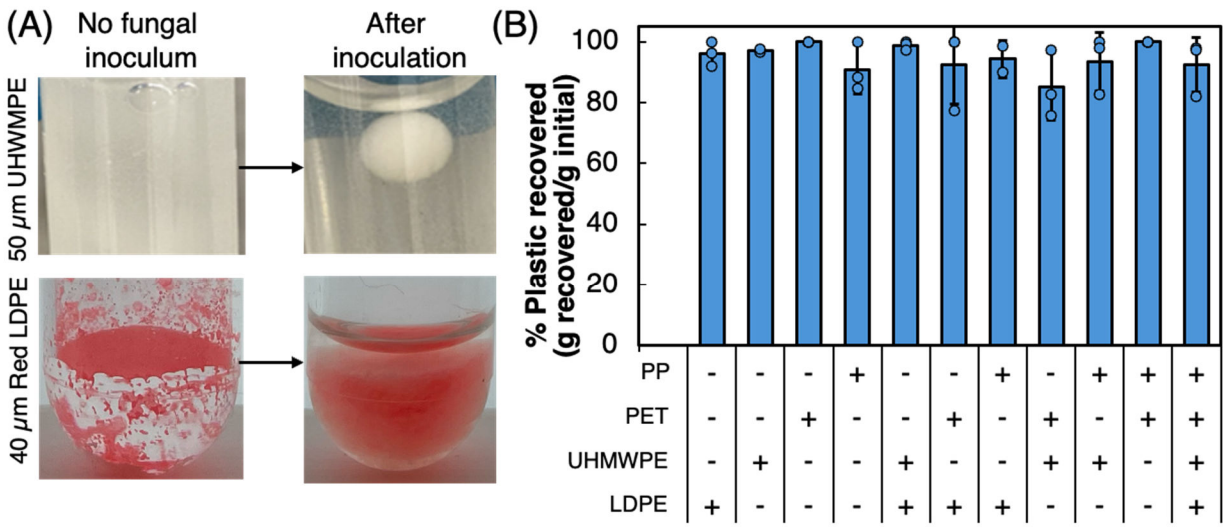

Figure 1: **Novel fungal isolate ubiquitously capture microplastics from solution**. (A) Polyethylene particles captured from solution via flocculation by fungal isolate; 50 μm UHMWPE particles (top) and ~40 μm red fluorescent LDPE beads (bottom) were used to demonstrate microplastics binding. The images in the left hand panels represent ultra-high molecular weight polyethylene (UHMWPE) particles in suspension (top) and red fluorescent low-density polyethylene (LDPE) particles (bottom) sitting at the air liquid interface or stuck to culture tube walls. After addition of the fungal inoculum, the microplastic particles attach to fungal hyphae, becoming embedded into the mycelium. The images on the right hand side are fungal mycelia with embedded microplastic particles, UHMWPE (top) and RLDPE (bottom). (B) Microplastics recovery of a variety of 'pristine' and post-consumer plastics shows ubiquitous recovery near 100%. Microplastics recovery was calculated by subtracting the remaining, un-flocculated plastic mass from the initial mass, dividing that by the total initial mass, and multiplying by 100%. Error bars represent standard error across three replicates.

Microplastics flocculation is common amongst *Aspergillus* species.

We acquired the whole genome for our microplastic-flocculating isolate and taxonomically placed it as an *Aspergillus* though phylogenetic analysis of its internal transcribed spacer (ITS) (Fig. 2a). The strain was identified as *Aspergillus fumigatus* due to grouping with published *Aspergillus fumigatus* genomes on a species tree constructed using OrthoFinder FastTree[58–60,64,65] and was thus named *Aspergillus fumigatus* UD1, hereafter referred to as AF-UD1 (Fig. 2b). Having identified our isolate, we next asked if this ability for microplastics colonization was conserved across the genus by assessing five common *Aspergillus* species spanning a range of phylogenetic distances from AF-UD1 (Fig 2). Each strain successfully flocculated microplastics between 1-5 g of plastic per g of dry biomass (Fig. 3). The recovery of microplastics by all strains implies that there are conserved molecular phenomena occurring in *Aspergilli* cultures that permit microplastics capture.

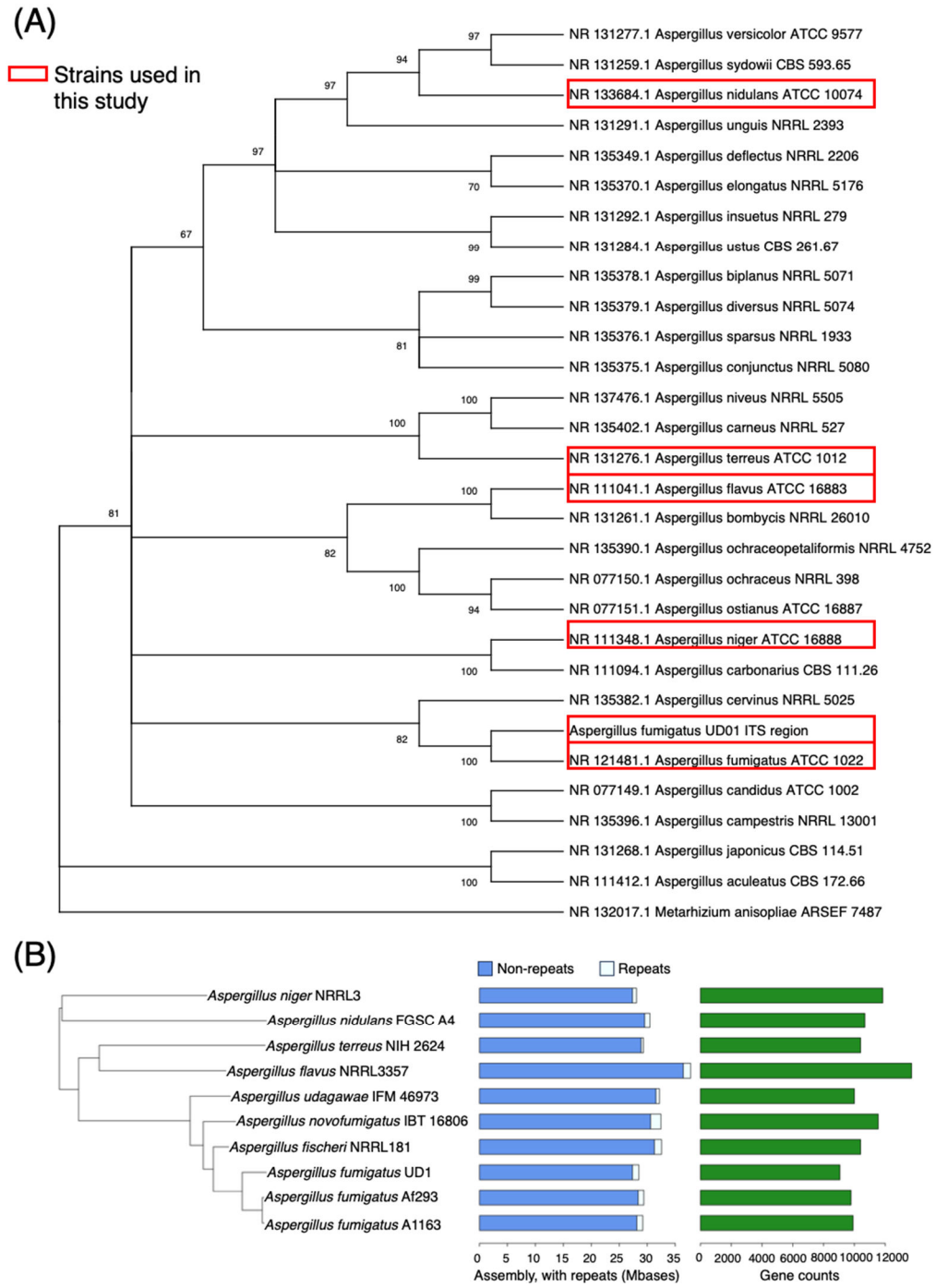

Figure 2: Novel plastics-flocculating isolate from mealworm gut is an *Aspergillus* (A) Phylogenetic tree of 45 *Aspergillus* strains built using complete ITS sequences, with strains used in this study boxed in red. A neighbor joining tree was constructed with 100 bootstrap iterations with ClustalW alignment, using *Metarhizium anisopliaei* as the outgroup. Tree is rooted to the outgroup. (B) Species tree confirming taxonomic identification of AF UD1. The tree was built by FastTree based on orthofinder clustering.

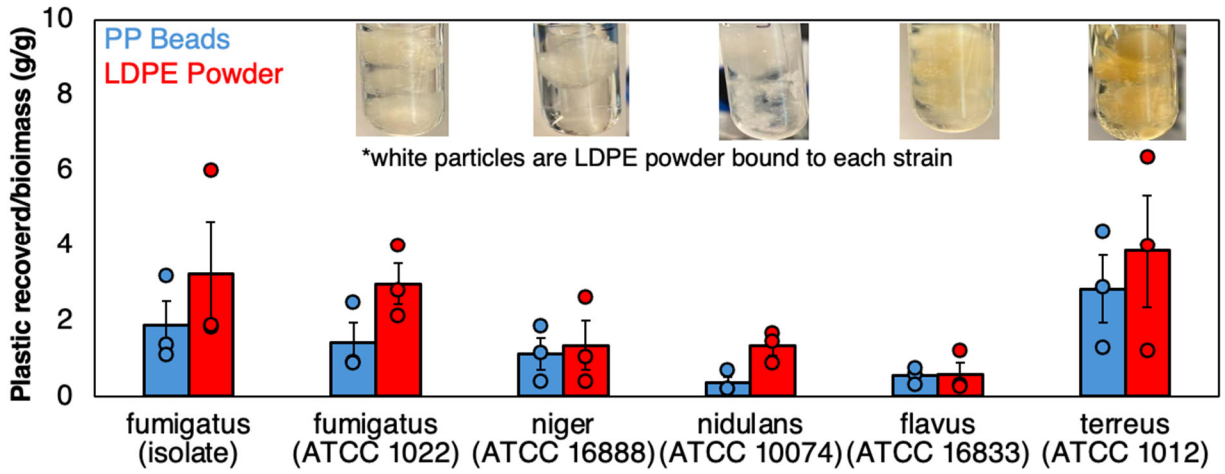

Figure 3: Plastics flocculation is conserved across *Aspergilli* Biomass normalized flocculation of two plastic types by *Aspergillus* strains across the genus. Mass of flocculated plastic was calculated by subtracting the mass of remaining plastic from the initial plastic mass. Images above each bar are 5 mL liquid cultures of each strain with flocculated ~200 µm goodfellow LDPE particles. Error bars represent standard error across three independent measurements

Microplastics flocculation is driven by redox-sensitive protein interactions

Confocal and scanning electron microscope (SEM) were used to observe microplastics flocculation and better understand underlying molecular phenomena. Microplastic particles are embedded both on the AF-UD1 surface and within the hyphal network (Fig. 4A, Supplementary movie). SEM images show a dense network of hyphae and extracellular polymeric substances (EPS) that pull plastic particles into the AF-UD1 network (Fig. 4B). The dense EPS and embedded nature of the microplastics formed by AF-UD1 creates a stable floc that can be mechanically perturbed without a loss of plastic. The formation of robust biofilm suggests that microplastics are pulled into the fungal matrix through hydrophobic interactions with secreted or membrane bound chemicals or biomolecules produced by the fungus.

Aspergilli adhesion to extracellular surfaces is canonically driven by surface proteins[74]. Hydrophobins are a highly surface-abundant class of proteins in *Aspergillus*, that have surfactant-like properties, namely amphiphilicity, making them very likely candidates to bind to extremely hydrophobic plastics[43,74]. Moreover, hydrophobins are predominant proteins in the outermost hydrophobic layer[43,74] of *Aspergillus fumigatus* that form at hydrophobic/hydrophilic interfaces[75]. Hydrophobins are characterized by eight conserved cysteine residues that form disulfide bonds that are responsible for stabilizing a large, hydrophobic solvent exposed interface[75]. We disturbed these disulfide bonds using beta-mercaptoethanol (βME)[76], removing hydrophobins from the AF-UD1 surface, to determine if hydrophobins play a role in microplastic binding. Microplastics flocculation ability was eliminated upon the addition of βME to the culture, consistent with surface proteins such as hydrophobins that rely on disulfide bonds for structure being integral to microplastics recovery processes (Fig. 4C).

Hydrophobins are necessary for microplastics flocculation

The role of hydrophobins in microplastics flocculation was directly assessed by repeating microplastics flocculation assays using *Aspergillus fumigatus* strains with each hydrophobin

knocked out of the genome. The *Aspergillus fumigatus* genome encodes 7 different hydrophobin genes, each expressing a different hydrophobin[43]. Genes for hydrophobin expression are *RODA, RODB, RODC, RODD, RODE, RODG,* and *RODF*, corresponding to proteins RodA through RodF[43]. Knocking out each hydrophobin gene reduced microplastics flocculation by *Aspergillus fumigatus* (Fig. 5A). AFΔRodA, AFΔRodB, AFΔRodE, AFΔRodG, and total knockout strain AFΔRodA-G all showed statistically significant decreases in flocculation relative to wild type AF-UD1, with AFΔRodG and AFΔRodA-G failing to flocculate plastics entirely (Fig. 5A). Rod A and RodG likely play an integral role in microplastics flocculation due to the observed significant decreases. Importantly, the inhibition of microplastics flocculation by the total knockout strain (ΔRodA-G) indicates that hydrophobins are necessary for microplastics flocculation.

Hydrophobin knockout data suggest that hydrophobins are necessary for microplastics flocculation, but use of purified hydrophobin in isolation of the host is necessary to confirm their propensity for microplastic flocculation. We thus expressed RodA, reported as the hydrophobin in *A. fumigatus* responsible for cell wall surface hydrophobicity[43], in the heterologous host *Yarrowia lipolytica* and subsequently purified the protein (purity confirmed via SDS-PAGE, Supplementary Fig. 3) to directly assess the microplastics flocculation ability by RodA in the absence of the host organism. Pure RodA flocculated microplastics from solution (Fig. 5B). Initially, green LDPE (GLDPE) particles sit atop the water due to their lower density than water and purified RodA resides in the bottom of the tube due to a density greater than that of water. GLDPE particles aggregate in that area after shaking, becoming entrapped in the purified hydrophobin, demonstrated by green particles near the bottom of the tube, below the air-liquid interface. Microplastics recovery by pure RodA and supporting hydrophobin knockout data demonstrate that hydrophobins are essential for microplastics flocculation by *Aspergilli*.

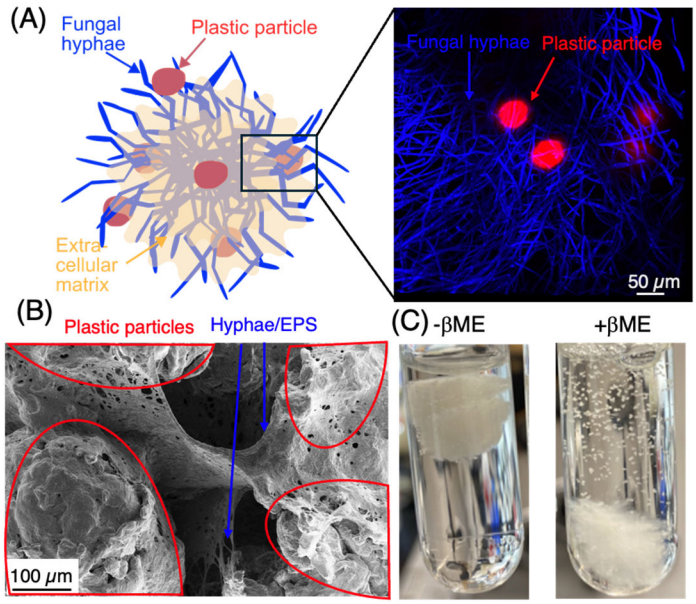

Figure 4: Hydrophobins drive microplastics flocculation in *Aspergilli*. (A) Confocal microscopy image of *Aspergillus fumigatus* AF-UD1 (blue) stained with calcofluor white using hyphal interactions to grab ~40 μm red fluorescent LDPE beads (red). (B) SEM image showing dense hyphal network of *Aspergillus fumigatus* AF-UD1 holding ~200 μm goodfellow LDPE microplastic particles in a floc. (C) Images showing ~200 μm goodfellow LDPE microplastics flocculation by AF-UD1 in the absence (left) and no flocculation in the presence (right) of beta-mercaptoethanol.

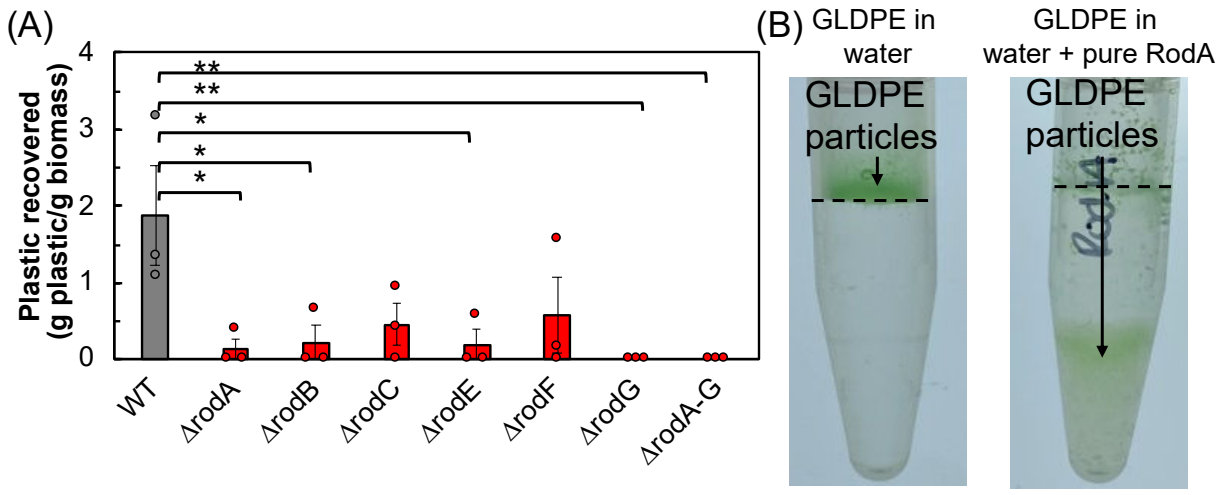

Figure 5: Hydrophobins are responsible for microplastics flocculation by AF-UD1. (A) Microplastics flocculation by *Aspergillus* strains with hydrophobin genes knocked out from the genome. *Aspergillus fumigatus* strains with each hydrophobin gene knocked out have reduced flocculation ability, indicating the importance of hydrophobins in microplastics recovery. Statistical significance testing was performed using a 2-tailed, homoscedastic t-test. * indicates p-value < 0.1, ** indicates p-value <0.05. (B) Recovery of ~40 µm green fluorescent LDPE beads by pure RodA (right) relative to a water control (left). After the addition of RodA, microplastic particles stick to the hydrophobin and are pulled from the air-water interface (dashed) to the bottom of the tube where the RodA sits.

Discussion:

Understanding microplastics colonization is essential to mitigate toxic xenobiotic leaching, greenhouse gas emissions, biodiversity effects caused by microplastics accumulation, and animal health defects caused by foreign and/or pathogenic microorganisms entering the food chain through microplastic-bound biofilms. In this study, we evaluate *Aspergillus* as a model genus of fungi to better understand fungal interactions with microplastics due to their ubiquity across soil and marine microbial communities[46,47] and potential for microplastics remediation through strong binding interactions. We showed that *Aspergilli* are efficient microplastics binding and recovery agents. We verified that the microplastics binding phenotype is conserved across the genus by demonstrating microplastics recovery with a subset of *Aspergilli* across 5 sub-genera: *Fumigati, Nidulantes, Wentii, Terrei, and Nigri*[77]. These strains each contain 5-8 hydrophobins, each between 10-20 kDa in size and containing 8-10 disulfide bond-forming cysteines that lead to amphiphilicity[48]. This conservation in hydrophobin abundance and size suggests that there are analogous hydrophobins in each species that contribute to the conserved surface hydrophobicity and microplastics binding phenotype. Our data also suggest that microplastics binding and capture occurs independent of plastic type and size, capturing all single and mixed plastics with nearly 100% recovery, consistent with previous studies detailing 100% recovery of 200 nm PS and 5µm PMMA by *Aspergillus niger*[45]. We also demonstrate flocculation of weathered PVC particles, implying that microplastic flocculation is also effective on plastics representative of those in the environment. This plastic type-independent microplastics binding is consistent with reports

that biofilm taxonomic composition does not vary with plastic type[78]. Rather, environmental factors such as temperature, pH, and salinity drive microplastics binding interactions and dictate which taxa persist in microplastic microbial communities[34]. Microplastics binding interactions require hydrophobic interactions between the microorganism and hydrophobic microplastic surface[79,80], meaning that any mechanism altering surface hydrophobicity would be agnostic to plastic type. However, we note that this reliance on hydrophobic interactions means that hydrophobins do not exclusively bind to plastics. *A. fumigatus* flocculates cellulose acetate similarly to microplastics, demonstrating that hydrophobin binding is not specific to microplastics (Supplementary Fig. 2). Thus, competitive binding of alternative should be considered when deploying hydrophobins for microplastic capture in practice.

Microplastic-bound biofilms have historically been studied by identifying the dominant bacterial members present[27,33,35,78], overlooking the role of the biomolecules that drive colonization and the contributions of fungal biofilm species[36,44]. We demonstrate that hydrophobins are important to microplastics binding by showing a decrease in microplastics flocculation upon knockout of each hydrophobin gene out of the genome. More importantly, we showed that pure RodA, the most abundant *A. fumigatus* hydrophobin, flocculates microplastics in isolation from the host organism, demonstrating that pure hydrophobin proteins bind directly to microplastic particles and flocculate them. The discovery of this relationship between hydrophobins and microplastics in *Aspergillus* biofilms allows for advances in microplastics remediation, pathogenicity, and biodeconstruction efforts by providing the physiological context in which *Aspergilli* bind to biofilms. Understanding how these microplastic-fungi interactions form can allow for new hydrophobin-based technologies to capture microplastics, alleviating toxic leaching[10] and greenhouse gas emissions[11] caused by their accumulation. Moreover, technologies can arise to reverse binding, thereby mitigating diseases throughout the food chain caused by microplastic mediated pathogen transport such as in coral reefs[32], to fish[31], and to humans[24,29,43]. Moreover, the mitigation of fungal biofilm formation on microplastics can decrease threats to biodiversity from the travel of invasive species to new ecosystems via microplastics transport[26,81].

Due to their inherent hydrophobicity, hydrophobins have been shown to interact with plastic substrates, namely in the context of biological deconstruction of hydrolyzable plastics by fungal enzymes. For example, *Aspergillus oryzae* expresses hydrophobin RolA that recruits a cutinase that hydrolyses polybutylene-succinate-coadipate[51,82]. Moreover, RolA incubation with PET substrate prior to treatment with a PETase improved PET deconstruction from 17% to 26% weight loss[83]. While these studies have focused on fungal enzymes and natural complexing with hydrophobins, we detail efficient microbial microplastics binding via hydrophobins. Our work highlights one strategy by which microbes colonize suspended microplastic particles, which would be the first step of biological deconstruction. Engineering this process may lead to more efficient/rapid plastics bioconstruction. For example, PET deconstruction by a PETase was improved 328-fold relative to pure PETase and 9-fold relative to surface displayed PETase by co-displaying the PETase with HFBI, a hydrophobin from *T. reesei*, on heterologous host *Pichia pastoris*[50]. The work presented in this manuscript can build on such studies by providing a library of hydrophobins for plastics binding from *Aspergilli* that can be used to similarly enhance biological (micro)plastic deconstruction efforts.

Biologically compatible (micro)plastics binding technologies further enhance bioremediation efforts by providing a microplastics capture mechanism that interfaces with (bio)deconstruction efforts. Existing microplastics capture technologies used in wastewater treatment plants (WWTPs), an extremely large source of microplastics[84], such as ultrafiltration, reverse osmosis, and chemical flocculation fail to provide a mechanism through which plastics can be deconstructed. Without conversion of (micro)plastics waste into non-plastic, non-toxic products,

the (micro)plastics waste crisis remains unresolved. Importantly, plastics wastes need to be upcycled into consumer products or recycled into plastics of equal value to the recycled waste to meet economic demands required to compete with plastics production from petrochemical refining[85]. Hydrophobins can thus be used to capture microplastics from aqueous environments with nearly 100% efficiency and can be utilized concurrently to engineer improved biological plastics deconstruction technologies that may be able to circumvent economic barriers with conventional mechanical or chemical plastics recycling[85]. Continued research on the interactions between fungal systems and microplastics is essential to identify hydrophobins capable of increased plastic binding that can ultimately be used to develop biological plastics deconstruction technologies that can mitigate the (micro)plastics waste accumulation crisis.

Environmental Implications:

The exponentially increasing accumulation of plastics in the environment leads to the direct release of toxic compounds such as xenobiotics and increased emission of greenhouse gases as a result of their environmental degradation[10,11]. Environmental plastics degradation generates microplastic particles that exacerbate these negative effects by leading to the distribution of microplastics particles to waterways and soil throughout the globe[12,15]. This widespread transport leads to microplastics ingestion by animals that is linked to negative health consequences such as hepatic lipid disorder and bile acids metabolism disorder in mice, inflammation and metabolism disruption in zebrafish[13,86], among other animal health impacts, directly contributing to food chain disruption by increasing mortality rates and via trophic transfer can affect human health [3,69].. Moreover, microplastics serve as a vector for transport of microorganisms[26,80], meaning that microplastic ingestion can also lead to the delivery of pathogenic microbes to animal species through ingestion, leading to the spread of disease throughout animal populations [13]. Microplastic mediated microorganism transport also disrupts soil and marine microenvironments through the delivery of foreign microbes[26] that can be invasive[26] directly changing microbial communities. These changes in microbial community composition can lead to reduced growth and nutrient uptake by plants[87], thereby percolating changes through the food web again.

In this work, we demonstrate that hydrophobins can be used as a sustainable microplastics capture and removal agent. However, the direct use of pathogenic fungal strains for microplastics capture can lead to undesired environmental consequence such as the disruption of microbial community biodiversity from the introduction of a non-native strain. Moreover, pathogenic strains bound to unrecovered microplastic particles could proliferate in the environment, leading to further biodiversity and human health issues from their spread. Alternatively, non-pathogenic *Aspergillus* species can be used for microplastics capture, but fungal community sequencing should be carried out to ensure the species is already present in the microbial community in the area of remediation interest to limit biodiversity disruption. Additionally, fungal-microplastic floccs contain water, which could require processing to dry them, dependent on downstream needs. To limit environmental impacts and process economics concerns from drying, pure hydrophobins can be deployed in waterways or in water treatment facilities to capture microplastics due to their inert nature.. We have shown that hydrophobins can be used to remove microplastics from real-world environments such as water treatment plants or the ocean by confirming that microplastics capture is agnostic to both particle size and chemical identity and by demonstrating microplastics capture at concentrations ranging from 20-40 mg/mL, greater than those in marine environments[72,73]. While these data show the potential for microplastics remediation using pure hydrophobins, this is likely more costly than using an *Aspergillus* strain. Heterologous expression of a candidate hydrophobin in hosts such as *Y. lipolytica* or *P. pastoris* can limit downstream purification costs through the use of efficient secretion systems (cite). While we leave economic evaluation of hydrophobin based microplastic remediation technologies to future studies, this work

shows promise for hydrophobin based microplastics removal. This technology can lead to the alleviation of toxicity concerns from microplastics degradation and subsequently mitigating animal health and biodiversity consequences caused by their ingestion

Statement of Competing Interests:

Work from this manuscript is claimed under pending provisional patent 63/564,151

Acknowledgements:

This research was funded in part by the Chemistry Biology Interface at the University of Delaware, under NIH training grant T32GM133395. This research was funded in part by the Delaware Environmental Institute, University of Delaware. Reagents for this research were ordered in part with funds from the QIAGEN Young Scientist Research Grant award 2022. This material is based upon work supported by the U.S. Department of Energy, Office of Science, Office of Biological and Environmental Research under Award Numbers DE-SC0022018 and DE-SC0023085. The work (proposal: 10.46936/fics.proj.2021.60038/60000396) conducted by the U.S. Department of Energy Joint Genome Institute (https://ror.org/04xm1d337), a DOE Office of Science User Facility, is supported by the Office of Science of the U.S. Department of Energy operated under Contract No. DE-AC02-05CH11231. The Environmentally relevant PVC micronanoplastics used in the study are part of the Rutgers Envronmentally Relevant Micronanoplastic Repository housed at Rutgers Nanoscience and Advanced Materials Center which was established with funding from NIFA/USDA (Grant number 2023-67017-39267), and the NIH/NIEHS Research Grant #1 R01 ES036043-01A1.

A portion of this research was performed under the Facilities Integrating Collaborations for User Science (FICUS) program (proposal: 508042) and used resources at the DOE Joint Genome Institute (https://ror.org/04xm1d337) and the Environmental Molecular Sciences Laboratory (https://ror.org/04rc0xn13), which are DOE Office of Science User Facilities operated under Contract Nos. DE-AC02-05CH11231 (JGI) and DE-AC05-76RL01830 (EMSL). Sequencing Project ID: 1428900. Final Deliverable Project ID: 1428895. Microscopy access was supported by grants from the NIH-NIGMS (P20 GM103446), the NIGMS (P20 GM139760) and the State of Delaware. The Leica Stellaris 8 tauSTED/FLIM Confocal was acquired by NIIMBL, NIST (70NANB21H085) and the American Rescue Plan. We thank Debbie Powell and Sylvain Le Marchand for exceptional support on scanning electron microscopy and confocal microscopy, respectively..

Author Contributions (CRediT)

Ross R. Klauer: led all experimental work, investigation, methodology, validation, formal analysis, writing – original draft
Rachel Silvestri: investigation, methodology, writing – review and editing
Hanna White: investigation, writing – review and editing
Milton Das: methodology and investigation
Richard Hayes: methodology
Robert Riley: methodology
Anna Lipzen: methodology
Kerrie Barry: coordination
Igor V. Grigoriev: coordination
Jayson Talag: methodology
Victoria Bunting: methodology

Zachary Stevenson: investigation
Philip Demokritou: conceptualized part of the study, supervised part of the study, acquired funding, and reviewed & edited the manuscript.
Kevin Solomon: conceptualized the study, supervised the study, acquired funding, and reviewed & edited the manuscript.
Mark Blenner: conceptualized the study, supervised the study, acquired funding, and reviewed & edited the manuscript.

References

(1) Ma, H.; Pu, S.; Liu, S.; Bai, Y.; Mandal, S.; Xing, B. Microplastics in Aquatic Environments: Toxicity to Trigger Ecological Consequences. *Environmental Pollution* **2020**, *261*, 114089. https://doi.org/10.1016/j.envpol.2020.114089.

(2) Khalid, N.; Aqeel, M.; Noman, A.; Hashem, M.; Mostafa, Y. S.; Alhaithloul, H. A. S.; Alghanem, S. M. Linking Effects of Microplastics to Ecological Impacts in Marine Environments. *Chemosphere* **2021**, *264*, 128541. https://doi.org/10.1016/j.chemosphere.2020.128541.

(3) Yang, Z.; DeLoid, G. M.; Zarbl, H.; Baw, J.; Demokritou, P. Micro- and Nanoplastics (MNPs) and Their Potential Toxicological Outcomes: State of Science, Knowledge Gaps and Research Needs. *NanoImpact* **2023**, *32*, 100481. https://doi.org/10.1016/j.impact.2023.100481.

(4) Cary, C. M.; DeLoid, G. M.; Yang, Z.; Bitounis, D.; Polunas, M.; Goedken, M. J.; Buckley, B.; Cheatham, B.; Stapleton, P. A.; Demokritou, P. Ingested Polystyrene Nanospheres Translocate to Placenta and Fetal Tissues in Pregnant Rats: Potential Health Implications. *Nanomaterials (Basel)* **2023**, *13* (4), 720. https://doi.org/10.3390/nano13040720.

(5) DeLoid, G. M.; Yang, Z.; Bazina, L.; Kharaghani, D.; Sadrieh, F.; Demokritou, P. Mechanisms of Ingested Polystyrene Micro-Nanoplastics (MNPs) Uptake and Translocation in an *in Vitro* Tri-Culture Small Intestinal Epithelium. *Journal of Hazardous Materials* **2024**, *473*, 134706. https://doi.org/10.1016/j.jhazmat.2024.134706.

(6) DeLoid, G. M.; Cao, X.; Bitounis, D.; Singh, D.; Llopis, P. M.; Buckley, B.; Demokritou, P. Toxicity, Uptake, and Nuclear Translocation of Ingested Micro-Nanoplastics in an *in Vitro* Model of the Small Intestinal Epithelium. *Food and Chemical Toxicology* **2021**, *158*, 112609. https://doi.org/10.1016/j.fct.2021.112609.

(7) Bui, T. H.; Zuverza-Mena, N.; Kendrick, E.; Tamez, C.; Yadav, M.; Alotaibi, S.; Dimkpa, C.; DeLoid, G.; Sadik, O.; Demokritou, P.; White, J. C. Micro-Nanoscale Polystyrene Co-Exposure Impacts the Uptake and Translocation of Arsenic and Boscalid by Lettuce (*Lactuca Sativa*). *NanoImpact* **2025**, *37*, 100541. https://doi.org/10.1016/j.impact.2025.100541.

(8) Li, H.; Aguirre-Villegas, H. A.; Allen, R. D.; Bai, X.; Benson, C. H.; Beckham, G. T.; Bradshaw, S. L.; Brown, J. L.; Brown, R. C.; Cecon, V. S.; Curley, J. B.; Curtzwiler, G. W.; Dong, S.; Gaddameedi, S.; García, J. E.; Hermans, I.; Kim, M. S.; Ma, J.; Mark, L. O.; Mavrikakis, M.; Olafasakin, O. O.; Osswald, T. A.; Papanikolaou, K. G.; Radhakrishnan, H.; Sanchez Castillo, M. A.; Sánchez-Rivera, K. L.; Tumu, K. N.; Van Lehn, R. C.; Vorst, K. L.; Wright, M. M.; Wu, J.; Zavala, V. M.; Zhou, P.; Huber, G. W. Expanding Plastics Recycling Technologies: Chemical Aspects, Technology Status and Challenges. *Green Chemistry* **2022**, *24* (23), 8899–9002. https://doi.org/10.1039/d2gc02588d.

(9) Andrady, A. L. Microplastics in the Marine Environment. *Mar Pollut Bull* **2011**, *62* (8), 1596–1605. https://doi.org/10.1016/j.marpolbul.2011.05.030.

(10) Mondal, S.; Subramaniam, C. Xenobiotic Contamination of Water by Plastics and Pesticides Revealed through Real-Time, Ultrasensitive, and Reliable Surface-Enhanced Raman Scattering. *ACS Sustainable Chem. Eng.* **2020**, *8* (20), 7639–7648. https://doi.org/10.1021/acssuschemeng.0c00902.

(11) Shen, M.; Huang, W.; Chen, M.; Song, B.; Zeng, G.; Zhang, Y. (Micro)Plastic Crisis: Un-Ignorable Contribution to Global Greenhouse Gas Emissions and Climate Change. *Journal of Cleaner Production* **2020**, *254*, 120138. https://doi.org/10.1016/j.jclepro.2020.120138.
(12) Wu, P.; Huang, J.; Zheng, Y.; Yang, Y.; Zhang, Y.; He, F.; Chen, H.; Quan, G.; Yan, J.; Li, T.; Gao, B. Environmental Occurrences, Fate, and Impacts of Microplastics. *Ecotoxicology and Environmental Safety* **2019**, *184*, 109612. https://doi.org/10.1016/j.ecoenv.2019.109612.
(13) Wang, J.; Peng, C.; Li, H.; Zhang, P.; Liu, X. The Impact of Microplastic-Microbe Interactions on Animal Health and Biogeochemical Cycles: A Mini-Review. *Science of The Total Environment* **2021**, *773*, 145697. https://doi.org/10.1016/j.scitotenv.2021.145697.
(14) Van Cauwenberghe, L.; Devriese, L.; Galgani, F.; Robbens, J.; Janssen, C. R. Microplastics in Sediments: A Review of Techniques, Occurrence and Effects. *Marine Environmental Research* **2015**, *111*, 5–17. https://doi.org/10.1016/j.marenvres.2015.06.007.
(15) Sridharan, S.; Kumar, M.; Bolan, N. S.; Singh, L.; Kumar, S.; Kumar, R.; You, S. Are Microplastics Destabilizing the Global Network of Terrestrial and Aquatic Ecosystem Services? *Environmental Research* **2021**, *198*, 111243. https://doi.org/10.1016/j.envres.2021.111243.
(16) Ragusa, A.; Svelato, A.; Santacroce, C.; Catalano, P.; Notarstefano, V.; Carnevali, O.; Papa, F.; Rongioletti, M. C. A.; Baiocco, F.; Draghi, S.; D'Amore, E.; Rinaldo, D.; Matta, M.; Giorgini, E. Plasticenta: First Evidence of Microplastics in Human Placenta. *Environment International* **2021**, *146*, 106274. https://doi.org/10.1016/j.envint.2020.106274.
(17) Hu, C. J.; Garcia, M. A.; Nihart, A.; Liu, R.; Yin, L.; Adolphi, N.; Gallego, D. F.; Kang, H.; Campen, M. J.; Yu, X. Microplastic Presence in Dog and Human Testis and Its Potential Association with Sperm Count and Weights of Testis and Epididymis. *Toxicological Sciences* **2024**, *200* (2), 235–240. https://doi.org/10.1093/toxsci/kfae060.
(18) Leslie, H. A.; van Velzen, M. J. M.; Brandsma, S. H.; Vethaak, A. D.; Garcia-Vallejo, J. J.; Lamoree, M. H. Discovery and Quantification of Plastic Particle Pollution in Human Blood. *Environment International* **2022**, *163*, 107199. https://doi.org/10.1016/j.envint.2022.107199.
(19) Chain (CONTAM), E. P. on C. in the F. Presence of Microplastics and Nanoplastics in Food, with Particular Focus on Seafood. *EFSA Journal* **2016**, *14* (6), e04501. https://doi.org/10.2903/j.efsa.2016.4501.
(20) Wright, S. L.; Kelly, F. J. Plastic and Human Health: A Micro Issue? *Environ. Sci. Technol.* **2017**, *51* (12), 6634–6647. https://doi.org/10.1021/acs.est.7b00423.
(21) Yang, Z.; DeLoid, G. M.; Baw, J.; Zarbl, H.; Demokritou, P. Assessment of Ingested Micro- and Nanoplastic (MNP)-Mediated Genotoxicity in an In Vitro Model of the Small Intestinal Epithelium (SIE). *Nanomaterials (Basel)* **2024**, *14* (9), 807. https://doi.org/10.3390/nano14090807.
(22) Kharaghani, D.; DeLoid, G. M.; Bui, T. H.; Zuverza-Mena, N.; Tamez, C.; Musante, C.; White, J. C.; Demokritou, P. Ingested Polystyrene Micro-Nanoplastics Increase the Absorption of Co-Ingested Arsenic and Boscalid in an In Vitro Triculture Small Intestinal Epithelium Model. *Microplastics* **2025**, *4* (1), 4. https://doi.org/10.3390/microplastics4010004.
(23) Kharaghani, D.; DeLoid, G. M.; He, P.; Swenor, B.; Bui, T. H.; Zuverza-Mena, N.; Tamez, C.; Musante, C.; Verzi, M.; White, J. C.; Demokritou, P. Toxicity and Absorption of Polystyrene Micro-Nanoplastics in Healthy and Crohn's Disease Human Duodenum-Chip Models.

Journal of Hazardous Materials **2025**, *490*, 137714. https://doi.org/10.1016/j.jhazmat.2025.137714.

(24) Marfella, R.; Prattichizzo, F.; Sardu, C.; Fulgenzi, G.; Graciotti, L.; Spadoni, T.; D'Onofrio, N.; Scisciola, L.; La Grotta, R.; Frigé, C.; Pellegrini, V.; Municinò, M.; Siniscalchi, M.; Spinetti, F.; Vigliotti, G.; Vecchione, C.; Carrizzo, A.; Accarino, G.; Squillante, A.; Spaziano, G.; Mirra, D.; Esposito, R.; Altieri, S.; Falco, G.; Fenti, A.; Galoppo, S.; Canzano, S.; Sasso, F. C.; Matacchione, G.; Olivieri, F.; Ferraraccio, F.; Panarese, I.; Paolisso, P.; Barbato, E.; Lubritto, C.; Balestrieri, M. L.; Mauro, C.; Caballero, A. E.; Rajagopalan, S.; Ceriello, A.; D'Agostino, B.; Iovino, P.; Paolisso, G. Microplastics and Nanoplastics in Atheromas and Cardiovascular Events. *New England Journal of Medicine* **2024**, *390* (10), 900–910. https://doi.org/10.1056/NEJMoa2309822.

(25) Ritchie, H.; Samborska, V.; Roser, M. *Plastic Pollution*. Our World in Data. https://ourworldindata.org/plastic-pollution (accessed 2024-06-04).

(26) Gaylarde, C. C.; de Almeida, M. P.; Neves, C. V.; Neto, J. A. B.; da Fonseca, E. M. The Importance of Biofilms on Microplastic Particles in Their Sinking Behavior and the Transfer of Invasive Organisms between Ecosystems. *Micro* **2023**, *3* (1), 320–337. https://doi.org/10.3390/micro3010022.

(27) Wu, X.; Pan, J.; Li, M.; Li, Y.; Bartlam, M.; Wang, Y. Selective Enrichment of Bacterial Pathogens by Microplastic Biofilm. *Water Research* **2019**, *165*, 114979. https://doi.org/10.1016/j.watres.2019.114979.

(28) Bowley, J.; Baker-Austin, C.; Porter, A.; Hartnell, R.; Lewis, C. Oceanic Hitchhikers – Assessing Pathogen Risks from Marine Microplastic. *Trends in Microbiology* **2021**, *29* (2), 107–116. https://doi.org/10.1016/j.tim.2020.06.011.

(29) Parsek, M. R.; Singh, P. K. Bacterial Biofilms: An Emerging Link to Disease Pathogenesis. *Annual Review of Microbiology* **2003**, *57* (Volume 57, 2003), 677–701. https://doi.org/10.1146/annurev.micro.57.030502.090720.

(30) Mammo, F. K.; Amoah, I. D.; Gani, K. M.; Pillay, L.; Ratha, S. K.; Bux, F.; Kumari, S. Microplastics in the Environment: Interactions with Microbes and Chemical Contaminants. *Science of The Total Environment* **2020**, *743*, 140518. https://doi.org/10.1016/j.scitotenv.2020.140518.

(31) Viršek, M. K.; Lovšin, M. N.; Koren, Š.; Kržan, A.; Peterlin, M. Microplastics as a Vector for the Transport of the Bacterial Fish Pathogen Species *Aeromonas Salmonicida*. *Marine Pollution Bulletin* **2017**, *125* (1), 301–309. https://doi.org/10.1016/j.marpolbul.2017.08.024.

(32) Lamb, J. B.; Willis, B. L.; Fiorenza, E. A.; Couch, C. S.; Howard, R.; Rader, D. N.; True, J. D.; Kelly, L. A.; Ahmad, A.; Jompa, J.; Harvell, C. D. Plastic Waste Associated with Disease on Coral Reefs. *Science* **2018**, *359* (6374), 460–462. https://doi.org/10.1126/science.aar3320.

(33) Oberbeckmann, S.; Löder, M. G. J.; Labrenz, M. Marine Microplastic-Associated Biofilms – a Review. *Environ. Chem.* **2015**, *12* (5), 551–562. https://doi.org/10.1071/EN15069.

(34) Luo, H.; Liu, C.; He, D.; Xu, J.; Sun, J.; Li, J.; Pan, X. Environmental Behaviors of Microplastics in Aquatic Systems: A Systematic Review on Degradation, Adsorption, Toxicity and Biofilm under Aging Conditions. *Journal of Hazardous Materials* **2022**, *423*, 126915. https://doi.org/10.1016/j.jhazmat.2021.126915.

(35) He, S.; Jia, M.; Xiang, Y.; Song, B.; Xiong, W.; Cao, J.; Peng, H.; Yang, Y.; Wang, W.; Yang, Z.; Zeng, G. Biofilm on Microplastics in Aqueous Environment: Physicochemical Properties and Environmental Implications. *Journal of Hazardous Materials* **2022**, *424*, 127286. https://doi.org/10.1016/j.jhazmat.2021.127286.
(36) Yang, Y.; Liu, W.; Zhang, Z.; Grossart, H.-P.; Gadd, G. M. Microplastics Provide New Microbial Niches in Aquatic Environments. *Appl Microbiol Biotechnol* **2020**, *104* (15), 6501–6511. https://doi.org/10.1007/s00253-020-10704-x.
(37) Parrish, K.; L. Fahrenfeld, N. Microplastic Biofilm in Fresh- and Wastewater as a Function of Microparticle Type and Size Class. *Environmental Science: Water Research & Technology* **2019**, *5* (3), 495–505. https://doi.org/10.1039/C8EW00712H.
(38) Klausen, M.; Heydorn, A.; Ragas, P.; Lambertsen, L.; Aaes-Jørgensen, A.; Molin, S.; Tolker-Nielsen, T. Biofilm Formation by Pseudomonas Aeruginosa Wild Type, Flagella and Type IV Pili Mutants. *Molecular Microbiology* **2003**, *48* (6), 1511–1524. https://doi.org/10.1046/j.1365-2958.2003.03525.x.
(39) Pratt, L. A.; Kolter, R. Genetic Analysis of Escherichia Coli Biofilm Formation: Roles of Flagella, Motility, Chemotaxis and Type I Pili. *Molecular Microbiology* **1998**, *30* (2), 285–293. https://doi.org/10.1046/j.1365-2958.1998.01061.x.
(40) O'Toole, G.; Kaplan, H. B.; Kolter, R. Biofilm Formation as Microbial Development. *Annual Review of Microbiology* **2000**, *54* (Volume 54, 2000), 49–79. https://doi.org/10.1146/annurev.micro.54.1.49.
(41) Verstrepen, K. J.; Reynolds, T. B.; Fink, G. R. Origins of Variation in the Fungal Cell Surface. *Nat Rev Microbiol* **2004**, *2* (7), 533–540. https://doi.org/10.1038/nrmicro927.
(42) Willaert, R. G. Adhesins of Yeasts: Protein Structure and Interactions. *Journal of Fungi* **2018**, *4* (4), 119. https://doi.org/10.3390/jof4040119.
(43) Valsecchi, I.; Dupres, V.; Stephen-Victor, E.; Guijarro, J. I.; Gibbons, J.; Beau, R.; Bayry, J.; Coppee, J.-Y.; Lafont, F.; Latgé, J.-P.; Beauvais, A. Role of Hydrophobins in Aspergillus Fumigatus. *Journal of Fungi* **2018**, *4* (1), 2. https://doi.org/10.3390/jof4010002.
(44) Kettner, M. T.; Rojas-Jimenez, K.; Oberbeckmann, S.; Labrenz, M.; Grossart, H.-P. Microplastics Alter Composition of Fungal Communities in Aquatic Ecosystems. *Environmental Microbiology* **2017**, *19* (11), 4447–4459. https://doi.org/10.1111/1462-2920.13891.
(45) Wang, H.; Neal, B.; White, B.; Nelson, B.; Lai, J.; Long, B.; Arreola-Vargas, J.; Yu, J.; Banik, M. T.; Dai, S. Y. Microplastics Removal in the Aquatic Environment via Fungal Pelletization. *Bioresource Technology Reports* **2023**, *23*, 101545. https://doi.org/10.1016/j.biteb.2023.101545.
(46) Sen, K.; Sen, B.; Wang, G. Diversity, Abundance, and Ecological Roles of Planktonic Fungi in Marine Environments. *Journal of Fungi* **2022**, *8* (5), 491. https://doi.org/10.3390/jof8050491.
(47) Christensen, M.; Tuthill, D. E. Aspergillus: An Overview. In *Advances in Penicillium and Aspergillus Systematics*; Samson, R. A., Pitt, J. I., Eds.; Springer US: Boston, MA, 1986; pp 195–209. https://doi.org/10.1007/978-1-4757-1856-0_18.
(48) Jensen, B. G.; Andersen, M. R.; Pedersen, M. H.; Frisvad, J. C.; Søndergaard, I. Hydrophobins from Aspergillus Species Cannot Be Clearly Divided into Two Classes. *BMC Res Notes* **2010**, *3* (1), 344. https://doi.org/10.1186/1756-0500-3-344.

(49) Grünbacher, A.; Throm, T.; Seidel, C.; Gutt, B.; Röhrig, J.; Strunk, T.; Vincze, P.; Walheim, S.; Schimmel, T.; Wenzel, W.; Fischer, R. Six Hydrophobins Are Involved in Hydrophobin Rodlet Formation in Aspergillus Nidulans and Contribute to Hydrophobicity of the Spore Surface. *PLOS ONE* **2014**, *9* (4), e94546. https://doi.org/10.1371/journal.pone.0094546.
(50) Chen, Z.; Duan, R.; Xiao, Y.; Wei, Y.; Zhang, H.; Sun, X.; Wang, S.; Cheng, Y.; Wang, X.; Tong, S.; Yao, Y.; Zhu, C.; Yang, H.; Wang, Y.; Wang, Z. Biodegradation of Highly Crystallized Poly(Ethylene Terephthalate) through Cell Surface Codisplay of Bacterial PETase and Hydrophobin. *Nature Communications 2022 13:1* **2022**, *13* (1), 1–17. https://doi.org/10.1038/s41467-022-34908-z.
(51) Takahashi, T.; Maeda, H.; Yoneda, S.; Ohtaki, S.; Yamagata, Y.; Hasegawa, F.; Gomi, K.; Nakajima, T.; Abe, K. The Fungal Hydrophobin RolA Recruits Polyesterase and Laterally Moves on Hydrophobic Surfaces. *Molecular Microbiology* **2005**, *57* (6), 1780–1796. https://doi.org/10.1111/j.1365-2958.2005.04803.x.
(52) Garrido, S. M.; Kitamoto, N.; Watanabe, A.; Shintani, T.; Gomi, K. Functional Analysis of FarA Transcription Factor in the Regulation of the Genes Encoding Lipolytic Enzymes and Hydrophobic Surface Binding Protein for the Degradation of Biodegradable Plastics in *Aspergillus Oryzae*. *Journal of Bioscience and Bioengineering* **2012**, *113* (5), 549–555. https://doi.org/10.1016/j.jbiosc.2011.12.014.
(53) Hillman, E. T.; Li, M.; Hooker, C. A.; Englaender, J. A.; Wheeldon, I.; Solomon, K. V. Hydrolysis of Lignocellulose by Anaerobic Fungi Produces Free Sugars and Organic Acids for Two-Stage Fine Chemical Production with Kluyveromyces Marxianus. *Biotechnology Progress* **2021**, *37* (5), e3172–e3172. https://doi.org/10.1002/BTPR.3172.
(54) Puppo, C.; Voisin, T.; Gontero, B. *Genomic DNA extraction from the pennate diatom Asterionella formosa optimised for next generation sequencing.* protocols.io. https://dx.doi.org/10.17504/protocols.io.jytcpwn (accessed 2024-08-13).
(55) Vaser, R.; Sovic, I.; Nagarajan, N.; Sikic, M. Fast and Accurate de Novo Genome Assembly from Long Uncorrected Reads. *Genome Res.* **2017**, gr.214270.116. https://doi.org/10.1101/gr.214270.116.
(56) Grabherr, M. G.; Haas, B. J.; Yassour, M.; Levin, J. Z.; Thompson, D. A.; Amit, I.; Adiconis, X.; Fan, L.; Raychowdhury, R.; Zeng, Q.; Chen, Z.; Mauceli, E.; Hacohen, N.; Gnirke, A.; Rhind, N.; di Palma, F.; Birren, B. W.; Nusbaum, C.; Lindblad-Toh, K.; Friedman, N.; Regev, A. Full-Length Transcriptome Assembly from RNA-Seq Data without a Reference Genome. *Nat Biotechnol* **2011**, *29* (7), 644–652. https://doi.org/10.1038/nbt.1883.
(57) Grigoriev, I. V.; Nikitin, R.; Haridas, S.; Kuo, A.; Ohm, R.; Otillar, R.; Riley, R.; Salamov, A.; Zhao, X.; Korzeniewski, F.; Smirnova, T.; Nordberg, H.; Dubchak, I.; Shabalov, I. MycoCosm Portal: Gearing up for 1000 Fungal Genomes. *Nucleic Acids Research* **2014**, *42* (D1), D699–D704. https://doi.org/10.1093/nar/gkt1183.
(58) Emms, D. M.; Kelly, S. OrthoFinder: Phylogenetic Orthology Inference for Comparative Genomics. *Genome Biology* **2019**, *20* (1), 238. https://doi.org/10.1186/s13059-019-1832-y.
(59) Emms, D. M.; Kelly, S. STRIDE: Species Tree Root Inference from Gene Duplication Events. *Molecular Biology and Evolution* **2017**, *34* (12), 3267–3278. https://doi.org/10.1093/molbev/msx259.
(60) Emms, D. M.; Kelly, S. STAG: Species Tree Inference from All Genes. bioRxiv February 19, 2018, p 267914. https://doi.org/10.1101/267914.

(61) Revell, L. J. Phytools 2.0: An Updated R Ecosystem for Phylogenetic Comparative Methods (and Other Things). *PeerJ* **2024**, *12*, e16505. https://doi.org/10.7717/peerj.16505.
(62) Arnaud, M. B.; Cerqueira, G. C.; Inglis, D. O.; Skrzypek, M. S.; Binkley, J.; Chibucos, M. C.; Crabtree, J.; Howarth, C.; Orvis, J.; Shah, P.; Wymore, F.; Binkley, G.; Miyasato, S. R.; Simison, M.; Sherlock, G.; Wortman, J. R. The Aspergillus Genome Database (AspGD): Recent Developments in Comprehensive Multispecies Curation, Comparative Genomics and Community Resources. *Nucleic Acids Research* **2012**, *40* (D1), D653–D659. https://doi.org/10.1093/nar/gkr875.
(63) Skerker, J. M.; Pianalto, K. M.; Mondo, S. J.; Yang, K.; Arkin, A. P.; Keller, N. P.; Grigoriev, I. V.; Glass, N. L. Chromosome Assembled and Annotated Genome Sequence of Aspergillus Flavus NRRL 3357. *G3 Genes*|*Genomes*|*Genetics* **2021**, *11* (8), jkab213. https://doi.org/10.1093/g3journal/jkab213.
(64) Nierman, W. C.; Pain, A.; Anderson, M. J.; Wortman, J. R.; Kim, H. S.; Arroyo, J.; Berriman, M.; Abe, K.; Archer, D. B.; Bermejo, C.; Bennett, J.; Bowyer, P.; Chen, D.; Collins, M.; Coulsen, R.; Davies, R.; Dyer, P. S.; Farman, M.; Fedorova, N.; Fedorova, N.; Feldblyum, T. V.; Fischer, R.; Fosker, N.; Fraser, A.; García, J. L.; García, M. J.; Goble, A.; Goldman, G. H.; Gomi, K.; Griffith-Jones, S.; Gwilliam, R.; Haas, B.; Haas, H.; Harris, D.; Horiuchi, H.; Huang, J.; Humphray, S.; Jiménez, J.; Keller, N.; Khouri, H.; Kitamoto, K.; Kobayashi, T.; Konzack, S.; Kulkarni, R.; Kumagai, T.; Lafton, A.; Latgé, J.-P.; Li, W.; Lord, A.; Lu, C.; Majoros, W. H.; May, G. S.; Miller, B. L.; Mohamoud, Y.; Molina, M.; Monod, M.; Mouyna, I.; Mulligan, S.; Murphy, L.; O'Neil, S.; Paulsen, I.; Peñalva, M. A.; Pertea, M.; Price, C.; Pritchard, B. L.; Quail, M. A.; Rabbinowitsch, E.; Rawlins, N.; Rajandream, M.-A.; Reichard, U.; Renauld, H.; Robson, G. D.; de Córdoba, S. R.; Rodríguez-Peña, J. M.; Ronning, C. M.; Rutter, S.; Salzberg, S. L.; Sanchez, M.; Sánchez-Ferrero, J. C.; Saunders, D.; Seeger, K.; Squares, R.; Squares, S.; Takeuchi, M.; Tekaia, F.; Turner, G.; de Aldana, C. R. V.; Weidman, J.; White, O.; Woodward, J.; Yu, J.-H.; Fraser, C.; Galagan, J. E.; Asai, K.; Machida, M.; Hall, N.; Barrell, B.; Denning, D. W. Genomic Sequence of the Pathogenic and Allergenic Filamentous Fungus Aspergillus Fumigatus. *Nature* **2005**, *438* (7071), 1151–1156. https://doi.org/10.1038/nature04332.
(65) Fedorova, N. D.; Khaldi, N.; Joardar, V. S.; Maiti, R.; Amedeo, P.; Anderson, M. J.; Crabtree, J.; Silva, J. C.; Badger, J. H.; Albarraq, A.; Angiuoli, S.; Bussey, H.; Bowyer, P.; Cotty, P. J.; Dyer, P. S.; Egan, A.; Galens, K.; Fraser-Liggett, C. M.; Haas, B. J.; Inman, J. M.; Kent, R.; Lemieux, S.; Malavazi, I.; Orvis, J.; Roemer, T.; Ronning, C. M.; Sundaram, J. P.; Sutton, G.; Turner, G.; Venter, J. C.; White, O. R.; Whitty, B. R.; Youngman, P.; Wolfe, K. H.; Goldman, G. H.; Wortman, J. R.; Jiang, B.; Denning, D. W.; Nierman, W. C. Genomic Islands in the Pathogenic Filamentous Fungus Aspergillus Fumigatus. *PLOS Genetics* **2008**, *4* (4), e1000046. https://doi.org/10.1371/journal.pgen.1000046.
(66) Aguilar-Pontes, M. V.; Brandl, J.; McDonnell, E.; Strasser, K.; Nguyen, T. T. M.; Riley, R.; Mondo, S.; Salamov, A.; Nybo, J. L.; Vesth, T. C.; Grigoriev, I. V.; Andersen, M. R.; Tsang, A.; de Vries, R. P. The Gold-Standard Genome of Aspergillus Niger NRRL 3 Enables a Detailed View of the Diversity of Sugar Catabolism in Fungi. *Studies in Mycology* **2018**, *91* (1), 61–78. https://doi.org/10.1016/j.simyco.2018.10.001.
(67) Kjærbølling, I.; Vesth, T. C.; Frisvad, J. C.; Nybo, J. L.; Theobald, S.; Kuo, A.; Bowyer, P.; Matsuda, Y.; Mondo, S.; Lyhne, E. K.; Kogle, M. E.; Clum, A.; Lipzen, A.; Salamov, A.; Ngan,

C. Y.; Daum, C.; Chiniquy, J.; Barry, K.; LaButti, K.; Haridas, S.; Simmons, B. A.; Magnuson, J. K.; Mortensen, U. H.; Larsen, T. O.; Grigoriev, I. V.; Baker, S. E.; Andersen, M. R. Linking Secondary Metabolites to Gene Clusters through Genome Sequencing of Six Diverse Aspergillus Species. *Proceedings of the National Academy of Sciences* **2018**, *115* (4), E753–E761. https://doi.org/10.1073/pnas.1715954115.

(68) Kusuya, Y.; Takahashi-Nakaguchi, A.; Takahashi, H.; Yaguchi, T. Draft Genome Sequence of the Pathogenic Filamentous Fungus Aspergillus Udagawae Strain IFM 46973T. *Genome Announcements* **2015**, *3* (4), 10.1128/genomea.00834-15. https://doi.org/10.1128/genomea.00834-15.

(69) Personal communication with the authors of a manuscript under revision: Das, M.; Calderon, L.; Singh, D.; Majumder, S.; Bazina, L.; Vaze, N.; Trivanovic, U.; DeLoid, G.; Zeverza-Mena, N.; Kaur, M.; Konkol, J.; Tsilomelekis, G.; Sadik, O.; White, J.; Demokritou, P. Development and Characterization of Reference Environmentally Relevant Micro Nano-Plastics for Risk Assessment Studies. *NanoImpact, under revision* **2025**.

(70) Schwartz, C.; Shabbir-Hussain, M.; Frogue, K.; Blenner, M.; Wheeldon, I. Standardized Markerless Gene Integration for Pathway Engineering in Yarrowia Lipolytica. *ACS Synth. Biol.* **2017**, *6* (3), 402–409. https://doi.org/10.1021/acssynbio.6b00285.

(71) Pedersen, M. H.; Borodina, I.; Moresco, J. L.; Svendsen, W. E.; Frisvad, J. C.; Søndergaard, I. High-Yield Production of Hydrophobins RodA and RodB from Aspergillus Fumigatus in Pichia Pastoris. *Applied Microbiology and Biotechnology* **2011**, *90* (6), 1923–1932. https://doi.org/10.1007/S00253-011-3235-1/FIGURES/3.

(72) Lasee, S.; Mauricio, J.; Thompson, W. A.; Karnjanapiboonwong, A.; Kasumba, J.; Subbiah, S.; Morse, A. N.; Anderson, T. A. Microplastics in a Freshwater Environment Receiving Treated Wastewater Effluent. *Integrated Environmental Assessment and Management* **2017**, *13* (3), 528–532. https://doi.org/10.1002/ieam.1915.

(73) Guo, Y.; Xia, X.; Ruan, J.; Wang, Y.; Zhang, J.; LeBlanc, G. A.; An, L. Ignored Microplastic Sources from Plastic Bottle Recycling. *Science of The Total Environment* **2022**, *838*, 156038. https://doi.org/10.1016/j.scitotenv.2022.156038.

(74) Paris, S.; Debeaupuis, J.-P.; Crameri, R.; Carey, M.; Charlès, F.; Prévost, M. C.; Schmitt, C.; Philippe, B.; Latgé, J. P. Conidial Hydrophobins of Aspergillus Fumigatus. *Applied and Environmental Microbiology* **2003**, *69* (3), 1581–1588. https://doi.org/10.1128/AEM.69.3.1581-1588.2003.

(75) Sunde, M.; Kwan, A. H. Y.; Templeton, M. D.; Beever, R. E.; Mackay, J. P. Structural Analysis of Hydrophobins. *Micron* **2008**, *39* (7), 773–784. https://doi.org/10.1016/j.micron.2007.08.003.

(76) Smithies, O. Disulfide-Bond Cleavage and Formation in Proteins. *Science* **1965**, *150* (3703), 1595–1598. https://doi.org/10.1126/science.150.3703.1595.

(77) *Advances in Penicillium and Aspergillus Systematics*; Samson, R. A., Pitt, J. I., Eds.; Springer US: Boston, MA, 1986. https://doi.org/10.1007/978-1-4757-1856-0.

(78) Wright, R. J.; Erni-Cassola, G.; Zadjelovic, V.; Latva, M.; Christie-Oleza, J. A. Marine Plastic Debris: A New Surface for Microbial Colonization. *Environ. Sci. Technol.* **2020**, *54* (19), 11657–11672. https://doi.org/10.1021/acs.est.0c02305.

(79) Tang, H.; Cao, T.; Liang, X.; Wang, A.; Salley, S. O.; McAllister II, J.; Ng, K. Y. S. Influence of Silicone Surface Roughness and Hydrophobicity on Adhesion and Colonization of

Staphylococcus Epidermidis. *Journal of Biomedical Materials Research Part A* **2009**, *88A* (2), 454–463. https://doi.org/10.1002/jbm.a.31788.
(80) Sooriyakumar, P.; Bolan, N.; Kumar, M.; Singh, L.; Yu, Y.; Li, Y.; Weralupitiya, C.; Vithanage, M.; Ramanayaka, S.; Sarkar, B.; Wang, F.; Gleeson, D. B.; Zhang, D.; Kirkham, M. B.; Rinklebe, J.; M Siddique, K. H. Biofilm Formation and Its Implications on the Properties and Fate of Microplastics in Aquatic Environments: A Review. *Journal of Hazardous Materials Advances* **2022**, *6*, 100077. https://doi.org/10.1016/j.hazadv.2022.100077.
(81) Barnes, D. K. A. Invasions by Marine Life on Plastic Debris. *Nature* **2002**, *416* (6883), 808–809. https://doi.org/10.1038/416808a.
(82) Tanaka, T.; Nakayama, M.; Takahashi, T.; Nanatani, K.; Yamagata, Y.; Abe, K. Analysis of the Ionic Interaction between the Hydrophobin RodA and Two Cutinases of Aspergillus Nidulans Obtained via an Aspergillus Oryzae Expression System. *Applied Microbiology and Biotechnology* **2017**, *101* (6), 2343–2356. https://doi.org/10.1007/S00253-016-7979-5/FIGURES/5.
(83) Puspitasari, N.; Tsai, S.-L.; Lee, C.-K. Fungal Hydrophobin RolA Enhanced PETase Hydrolysis of Polyethylene Terephthalate. *Appl Biochem Biotechnol* **2021**, *193* (5), 1284–1295. https://doi.org/10.1007/s12010-020-03358-y.
(84) Murphy, F.; Ewins, C.; Carbonnier, F.; Quinn, B. Wastewater Treatment Works (WwTW) as a Source of Microplastics in the Aquatic Environment. *Environ. Sci. Technol.* **2016**, *50* (11), 5800–5808. https://doi.org/10.1021/acs.est.5b05416.
(85) Klauer, R. R.; Hansen, D. A.; Wu, D.; Monteiro, L. M. O.; Solomon, K. V.; Blenner, M. A. Biological Upcycling of Plastics Waste. *Annual Review of Chemical and Biomolecular Engineering* **2024,** 15:315-42. https://doi.org/10.1146/annurev-chembioeng-100522-115850.
(86) Zolotova, N.; Kosyreva, A.; Dzhalilova, D.; Fokichev, N.; Makarova, O. Harmful Effects of the Microplastic Pollution on Animal Health: A Literature Review. *PeerJ* **2022**, *10*, e13503. https://doi.org/10.7717/peerj.13503.
(87) Wang, W.; Ge, J.; Yu, X.; Li, H. Environmental Fate and Impacts of Microplastics in Soil Ecosystems: Progress and Perspective. *Science of The Total Environment* **2020**, *708*, 134841. https://doi.org/10.1016/j.scitotenv.2019.134841.

Supplementary information file for:

Hydrophobins from *Aspergillus* mediate fungal interactions with microplastics

Ross R. Klauer[1], Rachel Silvestri[1], Hanna White[1], Milton Das[2], Richard D. Hayes[3], Robert Riley[3], Anna Lipzen[3], Kerrie Barry[3], Igor V. Grigoriev[3,4], Jayson Talag[5], Victoria Mae Bunting[5], Zachary Stevenson[1], Philip Demokritou[2], Kevin V. Solomon[1]*, Mark Blenner[1]*

1 Chemical and Biomolecular Engineering, University of Delaware, 150 Academy St., Newark, DE 19716.

2 Nanoscience and Advanced Materials Center, Environmental and Occupational Health Sciences Institute, Rutgers University, 170 Frelinghuysen Road, Piscataway, New Jersey 08854

3U.S. Department of Energy Joint Genome Institute, Lawrence Berkeley National Laboratory, Berkeley, CA 94720

4 Department of Plant and Microbial Biology, University of California Berkeley, Berkeley, CA 94720

5 Arizona Genomics Institute, 1657 E Helen St, Tucson, AZ 85721

**Equal contribution, corresponding authors.*

Correspondence: blenner@udel.edu; kvs@udel.edu

Summary: 5 pages, 4 figures, 1 table

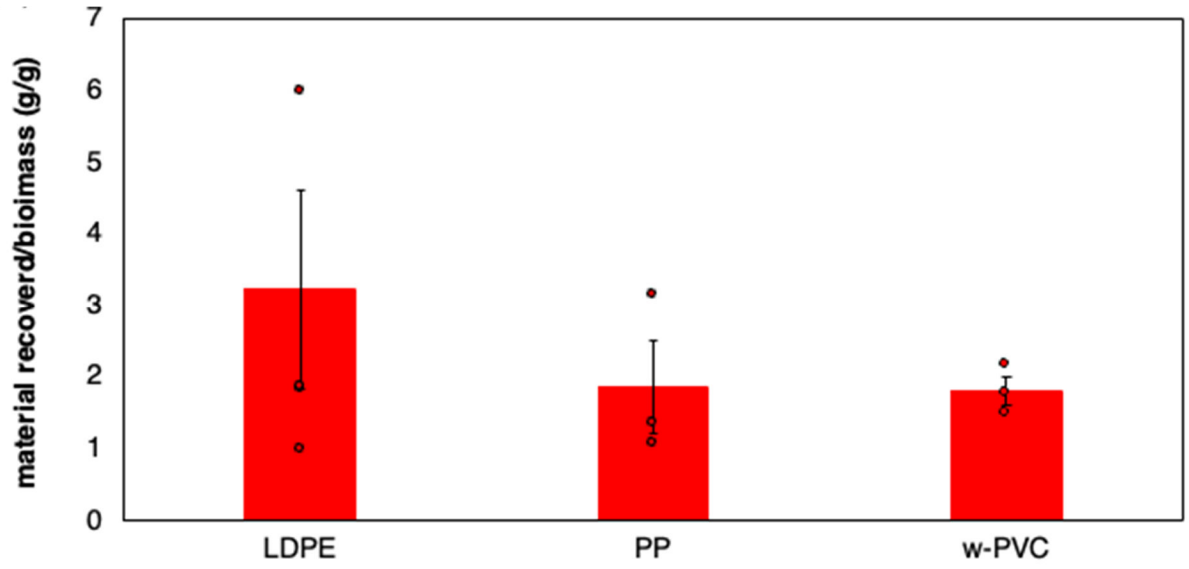

Supplementary Figure 1: AF-UD1 flocculation of weathered PVC particles. Biomass normalized flocculation of various plastics by AF-UD1. Mass of flocculated plastic was calculated by subtracting the mass of remaining plastic from the initial plastic mass. Error bars represent standard error across three independent measurements.

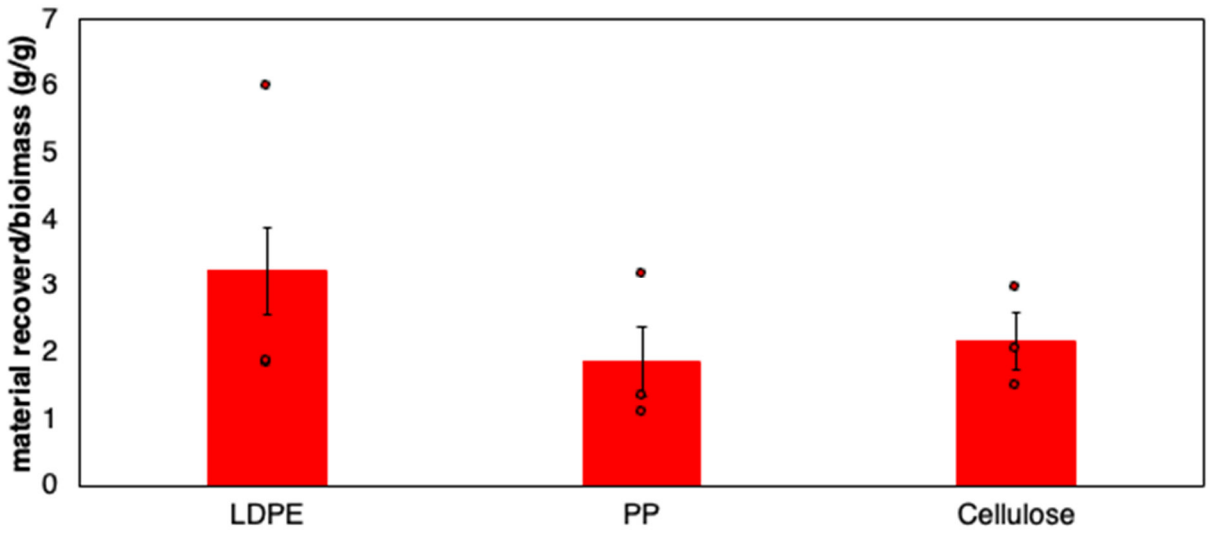

Supplementary Figure 2: AF-UD1 flocculation of cellulose acetate. Biomass normalized flocculation of various plastics and cellulose acetate by AF-UD1. Mass of flocculated material was calculated by subtracting the mass of remaining plastic from the initial plastic mass. Error bars represent standard error across three independent measurements.

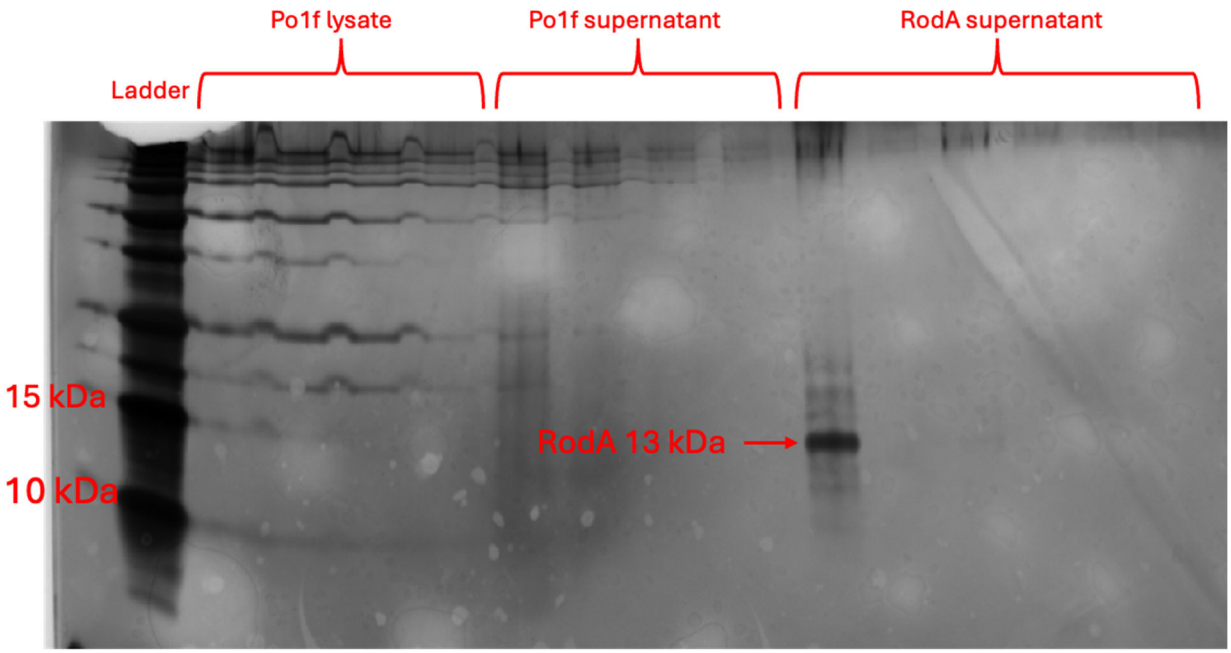

Supplementary Figure 3: SDS-PAGE of purified RodA from heterologous host *Y. lipolytica*. SDS-PAGE gel showing RodA after purification process from heterologous expression strain relative to wild-type po1f *Y. lipolytica* lysate supernatant that also went through the purification process. The leftmost lane of each sample represents the highest concentration of the sample, verified via BCA assay, where each subsequent lane in that sample set is a 2x dilution of the previous lane.

Supplementary Table 1: Concentrations in SDS-PAGE gel supplementary figure 2

Sample	Lane	Concentration (ng/µL)
WT po1f lysate	2	63
	3	21.5
	4	15.75
	5	7.875
WT po1f supernatant	6	99
	7	49.5
	8	24.75
	9	12.375
RodA supernatant	10	330
	11	165
	12	82.5
	13	41.25
	14	20.625
	15	10.3125

Codon optimized RodA sequence:

ATGAAGTTTAGCCTCTCTGCTGCAGTACTGGCCTTTGCCGTGTCTGTGGCTGCGCTCCCCC
AGCACGATGTCAACGCCGCTGGAAACGGTGTCGGCAACAAAGGCAATGCCAACGTGCGAT
TCCCTGTTCCCGACGACATCACCGTTAAACAAGCAACTGAGAAGTGTGGAGACCAGGCCC
AGCTGTCATGCTGCAACAAGGCCACCTACGCTGGCGACGTGACGGATATCGACGAGGGTAT
TCTGGCGGGTACTCTCAAGAACCTCATCGGCGGGGGCTCGGGAACAGAAGGACTAGGTTT
GTTCAACCAGTGTTCCAAGCTGGATCTGCAGATTCCTGTCATTGGCATCCCCATCCAGGCT
CTTGTTAACCAAAAGTGCAAGCAGAACATAGCCTGTTGCCAGAATTCGCCGTCCGACGCCA
GTGGCTCTCTGATTGGACTTGGTCTTCCATGTATTGCTCTGGGATCCATCTTGTAG

RodA protein sequence:

MKFSLSAAVLAFAVSVAALPQHDVNAAGNGVGNKGNANVRFPVPDDITVKQATEKCGDQAQLS
CCNKATYAGDVTDIDEGILAGTLKNLIGGGSGTEGLGLFNQCSKLDLQIPVIGIPIQALVNQKCKQ
NIACCQNSPSDASGSLIGLGLPCIALGSIL

NAMC REFERENCE ENP REPOSITORY

SUMMARY OF ENP PHYSICOCHEMICAL, BIOLOGICAL AND MORPHOLOGICAL CHARACTERIZATION

MNPs Information

Material:	PVC_CW_PM10: MD_030124-1
Description:	Cryo-milled & UV Weathered Polyvinyl Chloride Cryo-mill conditions: Cryo-milled 2 hours. UV weathering conditions: 0.55 W/m^2 at 340 nm at 65 °C for 21 days Particle diameter: PM_{10}.
Synthesis Date:	03-01-2024
Synthesis Method:	Cryo-mill at liquid N_2 temperature using a mechanical mill mm-400 and UV weathered using a Q-SUN Xenon Test Chamber Xe-1. (Appendix A for details)

Physical and chemical material characterization

Type	Method	Results	Remarks
Hydrodynamic Particle Size Distribution	Multi angle laser diffractions (MALD)	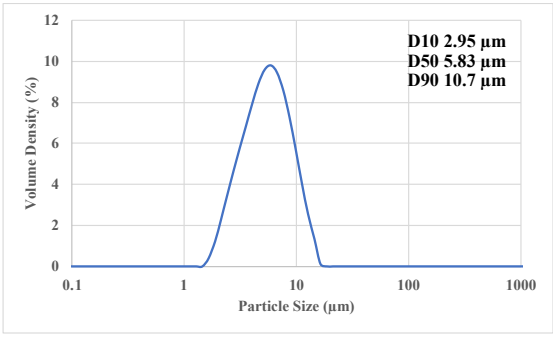	Particle size distribution peak at around 5.83 µm, D90 10.7 µm, which means 90% of the particle diameter are less 10.7 µm.
Primary Particle Size Distribution	Scanning electron microscopy (SEM)	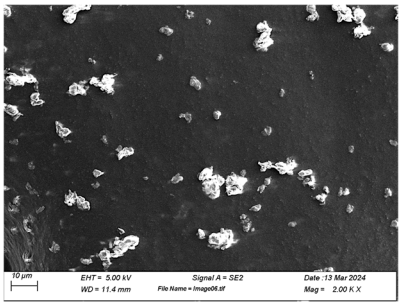 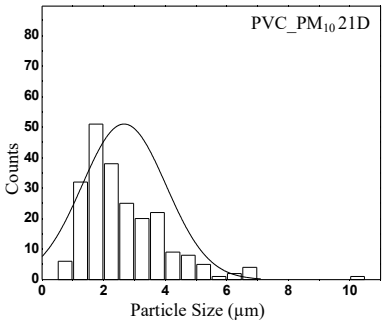	Particle size was determined using ImageJ and counted over 200 particles. Average particle size (2.7 ±1.4) µm.

Hydrophobicity	Contact Angle measurement	PVC_CW_PM10 #7990 = 142° #7991 = 132° #7992 = 149° 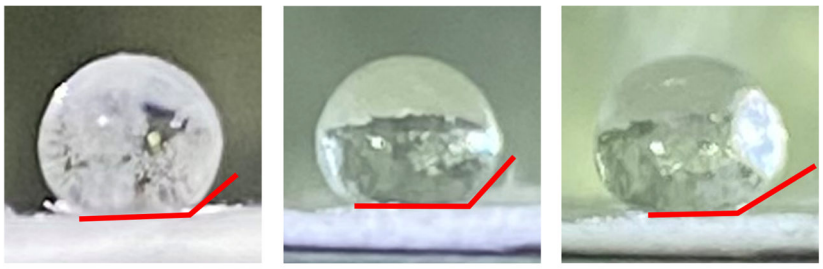	Cryo-milled PVC PM10 particles are hydrophobic as indicated by contact angle over 90°.
Surface Characterization	X-ray photoelectron spectroscopy (XPS)	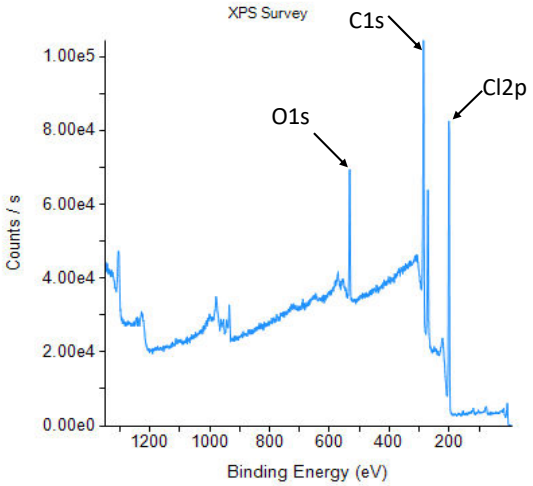	C - 66.5 % O - 11.1 % Cl - 20.5 % Other – 2.0%
	Fourier transform infra-red spectroscopy (FTIR)	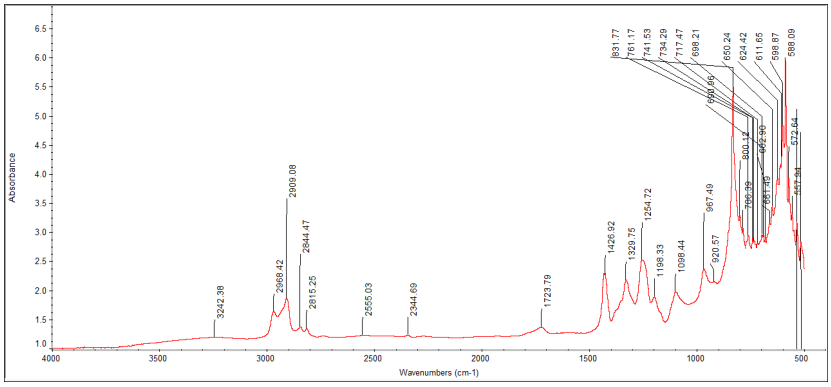	

Total elemental composition	Inductively Coupled Plasma Mass Spectrometry (ICP-MS)	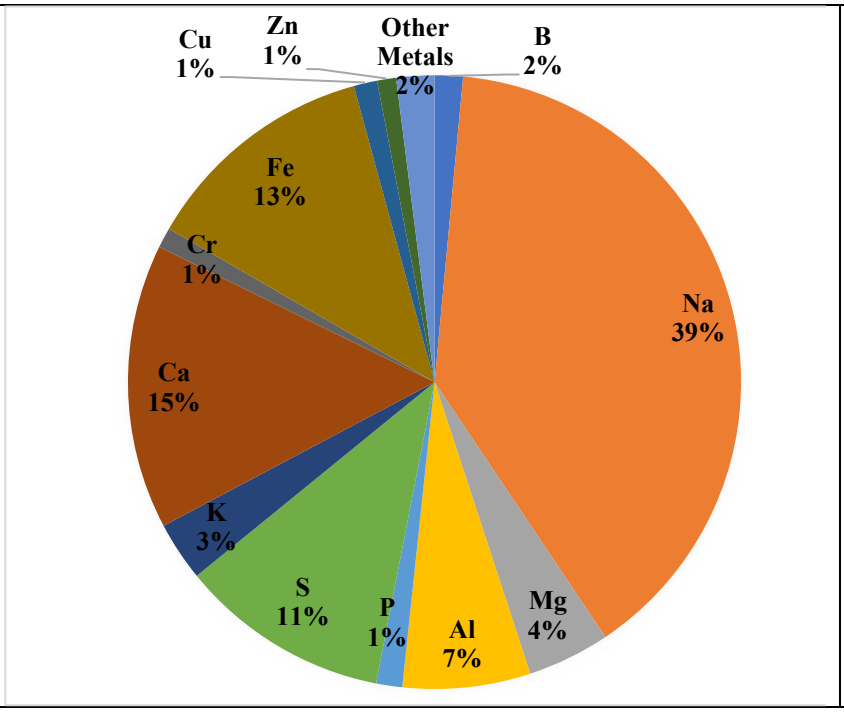	The total concentration of metal contaminants is 1.1% (w/w). The specific percentages of different metals within this 1.1% are depicted in the accompanying pie chart.

Biology			
Type	**Method**	**Results**	**Remarks**
Endotoxin	HEK-Blue LPS Detection Kit 2	0.12 EU/ml	Suspension Tested at 100 µg/ml
Sterility	Pharmacopeia Protocol for Sterility WHO Document QAS/11.413 FINAL	0 bacteria/mg 0 fungi/mg 0 total viable counts/mg	Suspension Tested at 100 µg/ml

APENDIX A: Synthesis details on the Cryo-milled PVC MNP powder PM_{10}:

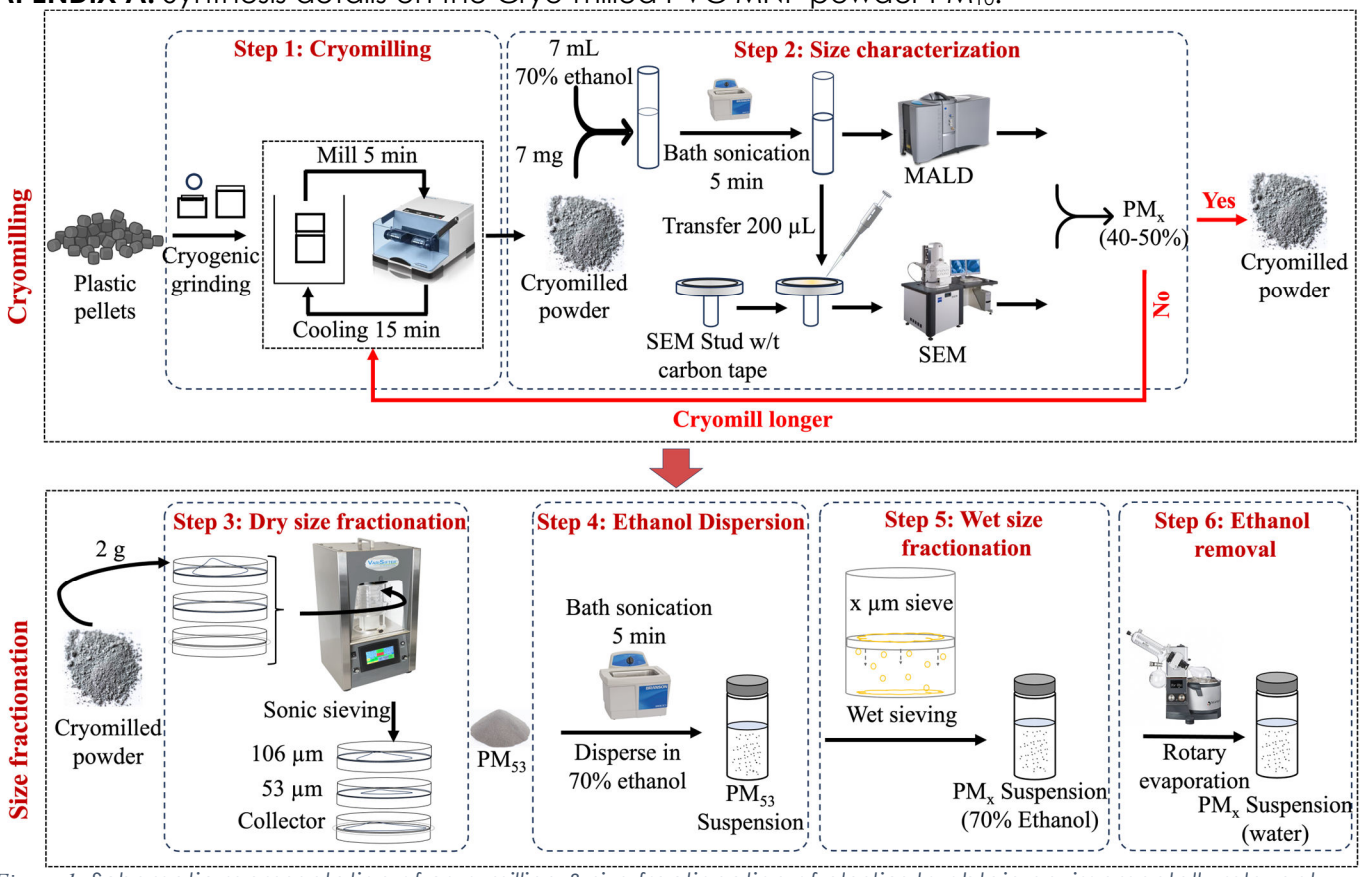

Figure 1: Schematic representation of cryo-milling & size fractionation of plastics to obtain environmentally relevant mechanically weathered MNPs.

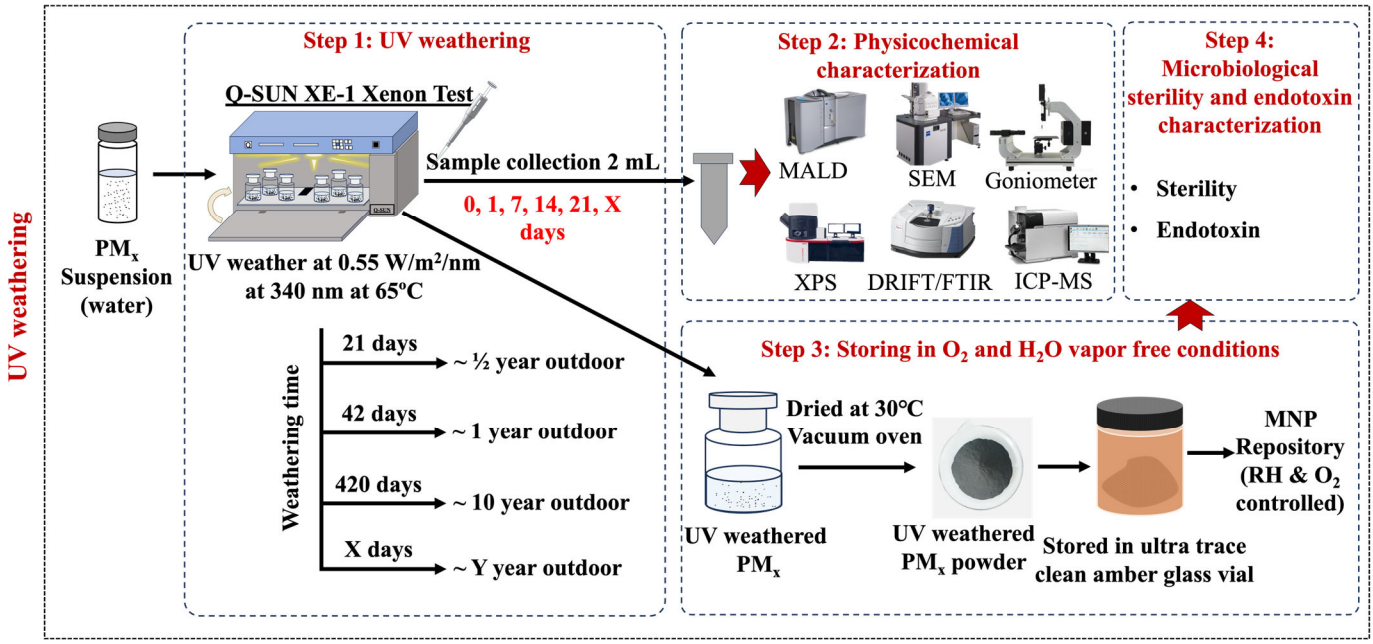

Figure 2: Schematic representation of UV-weathering of micro nano-plastics (MNPs).

Synthesis summary:

The lab-based mechanical degradation platform is illustrated in **Figure 1** and involves mechanical fragmentation by cryomilling and size fractionation by dry or wet approaches.

Cryomilling: Cryomilling was performed using a Retsch MM-400 mechanical milling device (Retsch, Haan, Germany), which is equipped with two 50 mL stainless-steel screw-top milling jars with stainless-steel 25 mm Ø grinding balls and can be programed to mill at 0-30 Hz for from 0 to 99 minutes. Eight grams of the plastic powder or pellets to be milled was added into each of the two 50 mL stainless-steel screw-top milling jars, along with the milling ball for each jar (**Figure 1, Step 1**). The milling jars were then submerged in liquid nitrogen for 15 minutes to lower the temperature of the jars and powder below the glass transition temperature of the plastic. The jars were then secured in the center of the Retsch MM 400, and the milling process was initiated at 30 Hz for 5 min. The milling jars were then again submerged in liquid nitrogen for 15 min and milling was performed for an additional 5 min. This process was repeated to achieve the required total milling time. The size distribution of the milled powder was determined as a function of cryomilling time (**Figure 1, Step 2**) using multi-angle light diffraction (MALD) and scanning electron microscopy (SEM). Another important parameter of the process is the "mass yield" as a function of cryomilling time. For example, if the target is to synthesize a powder in which 90% of the particles are below a desired size of x µm, an efficient mass yield of no less than 25% is desirable in order to produce a significant amount of material. Here, a mass yield of 25% was targeted for the cryomilling process for the eMNPs generated.

Size fractionation: Here, a combined sequential dry and wet sieving protocol was used for size fractionation. Details are provided in the SI.

Dry sieving: Dry sieving of the cryomilled powder was performed using a VS 1000 Varisifter sonic sieve (Advantech Manufacturing, New Berlin, WI) (**Figure 1, Step 3**). The milled plastic powder was applied to the top of the sieve stack, which included 106 µm, 53 µm, 10 µm, and 3 µm sieves, and a terminal fines (<3 µm) collector. The stack assembly was then placed in the VS 1000 test chamber and sonicated for one hour at 20 Hz. At the end of sonication, each stage of the stack, which had been pre-weighed, was weighed again to determine the quantity of material collected and the mass yield of each fraction. The cryomilled MNPs from each stage were collected in glass vials and were characterized as described below.

Wet sieving: The powder obtained from the terminal fines collector was subsequently processed by wet sieving in ethanol, which acts as a surfactant to help to disperse powder agglomerates. Due the hydrophobic nature of plastics, large agglomerates often form in the dry powder phase, making separation by dry sonication alone difficult. A wet size fractionation step using a surfactant is therefore necessary to effectively disperse and further fractionate the particles (**Figure 1, Steps 4-6**). Here, ethanol was used. It is worth noting that ethanol was removed after size separation using our recently developed protocols (see below). Specifically, 500 mg of the MNPs obtained from the terminal fines collector after dry sieving was added to a glass vial containing 50 mL of 70% ethanol, and the resulting mixture was subjected to bath sonication using a Branson M1800H bath sonicator (Branson Ultrasonics Corporation, Danbury, CT) for 5 minutes to achieve a homogeneous suspension (**Figure 1, Step 4**). Wet sieving of the ethanol suspension was then performed to obtain smaller sized MNP fractions (**Figure 1, Step 5**). To collect the particulate matter smaller than x µm (PMx), an x µm sized sieve (WS Tyler, Mentor, OH) was placed in a 1000 mL glass beaker, and 50 mL of the 70% ethanol suspension of MNP was applied

to the sieve using a transfer pipette (Cole-Parmer, Vernon Hills, IL). This procedure ensures that particles smaller than x µm would pass through the sieve and accumulate at the bottom of the beaker, while MNPs larger than x µm would be retained on the sieve. The sieve was then rinsed with an additional 10 mL of 70% ethanol, and the sieve passage was collected from the beaker. The yield of the wet sieving step was determined gravimetrically by placing 1 mL of the sieve passage in a pre-weighed aluminum foil weighing substrate, air drying in a fume hood, and re-weighing the substrate with dried PMx.

Removal of Ethanol: The ethanol was then removed and exchanged with water to create an aqueous suspension of PMx MNPs (**Figure 1, Step 6**) as described previously. 200 mL of PMx MNPs in 70% ethanol was added to a 1000 mL boiling flask. The flask was then attached to an electric rotary evaporator (Hydrion Scientific Instrument LLC, Vista, CA), and evaporated at 32 °C and 40 rpm until dry. One hundred mL of cell culture grade water (Cytiva, Logan, UT) was then added to the flask, and the mixture was bath sonicated for 5 min to disperse agglomerates and particles adherent to the flask. The flask was then returned to the rotary evaporator and evaporated at 32 °C and 40 rpm until dry. This process was repeated three times to ensure the complete removal of ethanol. The final aqueous suspension of MNPs was then transferred to a glass bottle. The flask was further rinsed with cell culture grade water and the rinsate was added to the bottle. A final MNP PMx concentration of approximately 15 mg/mL was targeted for the synthesized eMNPs.

UV weathering of the MNPs: The cryomilled MNPs were subsequently subjected to UV weathering (aging) (Figure 2) In order to weather the MNP PMx (**Figure 2, Step 1**), 30 mL of the aqueous MNP PMx suspensions, adjusted to 15 mg/mL, were transferred to 150 mL UV transparent glass bottles (Corning, Tewksbury, MA). The plastic caps of the glass bottles were replaced with UV-transparent 60 mm quartz petri dishes (Corning) to avoid weathering of the plastic caps, which could introduce unwanted MNPs to the samples, and to allow maximum UV radiation exposure of the samples. The bottles were then placed on the test specimen tray of a Q-SUN Xe-1 Xenon Arc Chamber (Q-Lab, Westlake, OH) and exposed under a UVA-340 lamp (Q-Lab) with irradiance set to 0.55 W/m^2/sec at 340 nm, and temperature set to 65 °C. At these settings, the Q-SUN accelerated UV weathering platform provides the equivalent of six months of outdoor sunlight exposure in 21 days (or 1 year in 42 days, or 10 years in 420 days). Sample suspensions were vortexed once a day to ensure uniform weathering of the particles. In order to assess the impacts of weathering on the physicochemical properties of the MNPs as a function of time, samples were collected at time 0 (no weathering) and after 1, 7, 14, and 21 days of weathering, for physicochemical analysis (**Figure 2, Step 2**), which included MALD and SEM to assess size distribution and morphology, and X-ray Photoelectron Spectroscopy (XPS) and Diffuse Reflectance Infrared Fourier Transform (DRIFT) to assess surface chemistry and modifications. Following UV weathering, samples were vacuum dried at 30 °C and the dried MNP powders were transferred to a trace clean amber glass vials (VWR) and stored in a humidity and oxygen-controlled glove box (**Figure 2, Step 3**). Stored samples were further characterized to assess hydrophobicity, metal contaminants, sterility, and endotoxin contamination (**Figure 2, Step 4**. The ethanol content of MNP powders was also assessed.